CHAPTER IV
FLY ASH AND NATURAL RUBBER LATEX MODIFIED RECYCLED AGGREGATE CONCRETE AS SUSTAINABLE RIGID PAVEMENT SURFACE

4.1 Introduction

The construction industry has increasingly embraced sustainable approaches to mitigate the environmental impact of infrastructure development (Hasan et al., 2024; Paul et al., 2024; Toy et al., 2025). The utilization of recycled materials has gained significant attention as an alternative to conventional raw materials, aligning with global efforts to promote circular economy practices. Among the various waste-derived materials, recycled concrete aggregate (RCA) has emerged as a viable substitute for natural aggregate (NA), e.g., fiber or nano-materials in concrete applications (Accornero et al., 2024; Reddy et al., 2024). The incorporation of RCA contributes to waste reduction by diverting construction and demolition waste from landfills while conserving natural resources. However, despite its advantages, RCA-based concrete often exhibits inferior mechanical properties compared to conventional concrete due to the porous nature of RCA and the presence of adhered cementitious mortar (Silva et al. 2014). Although RCA can be directly used to replace natural coarse aggregate, even at 100% replacement levels, numerous studies have reported reductions in strength, stiffness, and durability compared with natural aggregate concrete due to the attached mortar and higher porosity of RCA. Therefore, the incorporation of supplementary materials or modification techniques-such as fly ash, slag, or polymer latex-is often recommended to enhance the mechanical performance and long-term durability of RCA-based concrete, particularly for structural and pavement applications. These considerations highlight the need for optimizing RCA concrete through material modification to achieve a balance between sustainability and mechanical performance.

Natural rubber latex (NRL), an organic polymer obtained from Hevea brasiliensis, has demonstrated potential in improving the mechanical properties of RCA-based concrete. Due to its elastomeric nature, NRL contributes to enhanced flexibility, adhesion, and durability when incorporated into cementitious systems (Hoy et al. 2023). Previous research has highlighted its ability to modify the interfacial transition zone (ITZ) between aggregate and cement paste, thereby affecting compressive strength (f_c) and flexural strength (f_f) (Sukmak et al. 2020). Nevertheless, some studies have reported reductions in strength when higher dosages of NRL are used, as excessive latex content can disrupt cement hydration and lead to a porous matrix (Yaowarat et al. 2021). To address these limitations, the present study investigates the incorporation of fly ash (FA) as a pozzolanic material to refine the microstructure and enhance the long-term performance of NRL–RCA concrete.

FA, a byproduct of coal combustion in thermal power plants, has been extensively used in cement-based materials due to its ability to improve workability, strength, and durability (Knapen and Van Gemert 2015). As a supplementary cementitious material, FA undergoes a pozzolanic reaction with calcium hydroxide ($Ca(OH)_2$) released during cement hydration, forming additional calcium silicate hydrate (C-S-H) gel (Plank et al. 2015). This secondary hydration process enhances the density of the cement matrix, refines pore structure, and contributes to improved mechanical performance over time (Etxeberria et al. 2007). Several studies have demonstrated that FA incorporation enhances the compressive strength of RCA-based concrete by mitigating the adverse effects associated with RCA's porous nature and weak ITZ (Omary et al. 2016). Furthermore, the long-term benefits of FA, including reduced permeability and enhanced resistance to sulfate attack, make it a promising solution for addressing the durability concerns of RCA concrete (Arulrajah et al. 2015).

The application of FA in RCA-based concrete has been widely studied, yet limited research has explored its synergistic role with NRL in enhancing pavement concrete performance. In pavement applications, concrete is subjected to significant tensile and bending stresses, making flexural strength a critical parameter (Yaowarat et al. 2021). Previous studies have indicated that pozzolanic reactions associated with FA contribute to microstructural refinement, thereby improving bonding within the cementitious system (Nhieu et al. 2023). Moreover, the gradual strength development provided by FA can help offset the early-age reduction in strength often observed in NRL-modified concretes, potentially resulting in a more durable and resilient pavement material (Tran et al. 2022).

Another key aspect of FA incorporation is its impact on hydration kinetics and the overall microstructure of concrete. RCA, due to its previous exposure to hydration cycles, contains residual cementitious compounds that influence the hydration behavior of new cementitious matrix (Dilbas et al. 2014). The interaction between FA and RCA may lead to variations in reaction kinetics, affecting setting time, strength gain, and overall durability. Advanced analytical techniques, such as scanning electron microscopy (SEM), energy-dispersive X-ray spectroscopy (EDS), and X-ray diffraction (XRD), have been employed to evaluate the microstructural characteristics of RCA-based concrete (Behera et al. 2014). These methods provide insights into phase composition, elemental distribution, and the formation of hydration products, facilitating a deeper understanding of the mechanisms governing strength development in FA-modified NRL-RCA concrete (Buritatum et al. 2021; Buritatun et al. 2020).

In addition to mechanical performance, the environmental and economic implications of FA utilization warrant consideration. The increasing generation of FA as an industrial byproduct necessitates sustainable disposal solutions (Jansen et al. 2012). By integrating FA into concrete formulations, the construction sector can contribute to waste valorization while reducing the demand for Portland cement, which is associated with high carbon emissions (Plank et al. 2015). From an economic perspective, FA is often more cost-effective than ordinary Portland cement, making it a viable option for large-scale infrastructure projects (Ye et al. 2022). The combination of RCA, NRL, and FA thus presents an innovative approach to sustainable concrete production, aligning with global efforts to promote eco-friendly construction practices (Yaowarat et al. 2018; Yaowarat et al. 2019).

Despite the potential benefits, challenges associated with FA incorporation must be acknowledged. The variability in FA composition, influenced by factors such as coal source and combustion conditions, can impact its reactivity and performance in concrete (Omary et al. 2016). Furthermore, the optimal dosage of FA must be carefully determined to balance workability, early-age strength, and long-term durability. Excessive FA content may lead to delayed strength gain, which could pose limitations in applications requiring rapid construction cycles (Silva et al. 2014).

Another critical aspect in evaluating pavement materials is their behavior under cyclic or repeated loading. Unlike static tests, cyclic tests simulate the real service conditions of pavements, which are continuously subjected to traffic-induced stresses and fatigue over their service life. Parameters such as resilient modulus, permanent deformation, and flexural fatigue life provide essential insights into the long-term performance and durability of concrete materials under repeated loads (Werkmeister et al. 2004). However, limited research has investigated the cyclic performance of FA-modified NRL-RCA concrete. Addressing this gap is crucial for assessing the feasibility of such mixtures in pavement applications, where resistance to fatigue and deformation directly governs service life.

A comprehensive review of existing literature highlights the gap in research concerning the combined effect of FA and NRL in RCA-based concrete. While previous studies have investigated FA in RCA concrete and the benefits of NRL separately, limited research has explored their combined influence on f_c and f_f. Given the importance of these properties in pavement applications, this study aims to bridge the knowledge gap by systematically assessing the performance of FA-modified NRL-RCA concrete, thereby contributing to the development of sustainable and durable pavement materials.

By building upon the limitations of earlier studies, the present work advances the understanding of sustainable pavement concrete through a unified investigation of mechanical, fatigue, microstructural, and environmental behaviors. Whereas previous research has often examined fly ash or natural rubber latex separately, this study explores their combined effect within an RCA-based system specifically designed for rigid pavement applications. The research emphasizes the optimization of material proportions that satisfy Thai pavement strength standards while simultaneously minimizing CO_2 emissions and material costs. The findings are expected to offer practical guidelines for producing high-performance, low-carbon pavement concrete and to support the broader adoption of recycled aggregate technology in sustainable infrastructure development.

4.2 MATERIAL AND METHODS

4.2.1 Materials

Ordinary Portland cement (OPC) was utilized as the primary cementing material, possessing a specific gravity of 3.15. The detailed chemical composition of the Portland cement is presented in **Table 4.1.**

FA used in this research was sourced from a cement manufacturing plant in Nakhon Ratchasima Province, located in northeastern Thailand. According to its chemical composition (**Table 4.1**), FA contained 39.18% silicon dioxide (SiO_2), 22.64% aluminum oxide (Al_2O_3), and 15.45% iron oxide (Fe_2O_3), which are key contributors to its pozzolanic activity. With a high calcium oxide (CaO) content of 11.3%, the FA was classified as Class C in accordance with ASTM C618 (2019) standards. The specific gravity of FA was measured at 2.39, and the particle size distribution is illustrated in **Figure 4.1**.

Table 4.1 Chemical compositions of OPC and Fly Ash

Materials	Composition (%)						
	SiO_2	SO_3	Fe_2O_3	Al_2O_3	CaO	MgO	LOI
Cement	20.9	2.7	3.32	4.7	65.4	2.54	0.9
FA	39.18	4.29	15.45	22.64	11.3	1.69	1.61

River sand was selected as the fine aggregate in this study. Under a saturated surface dry (SSD) condition, it exhibited a specific gravity of 2.65. Additional properties of the sand included a water absorption capacity of 1.10%, a fineness modulus of 2.46, and a void content of 43.6%. The coarse aggregate used was recycled concrete aggregate (RCA), ranging in size from 4.75 to 19 mm. The RCA had a fineness modulus of 6.3 and a specific gravity of 2.67. It exhibited a water absorption rate of 5.5%, a porosity of 54%, and a Los Angeles abrasion value of 34%. A visual representation of the particle characteristics of both RCA and river sand is illustrated in **Figure 4.1.**

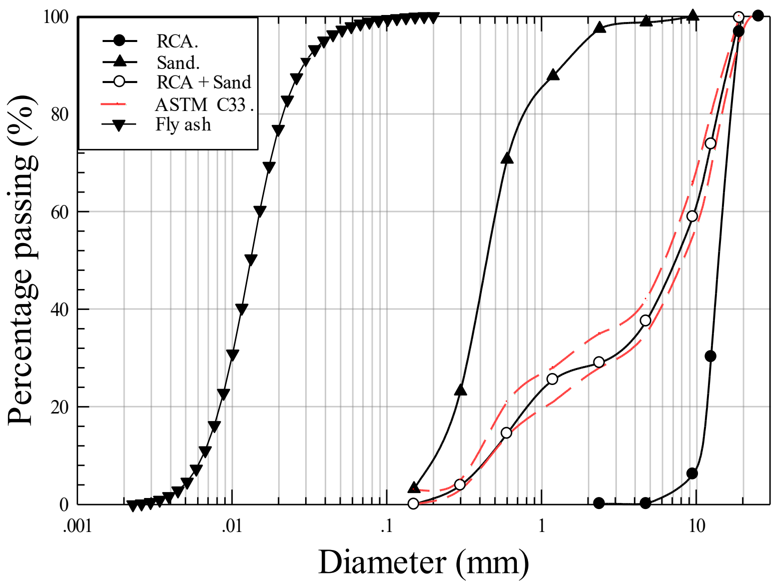

Figure 4.1 Particle size distributions of Sand, RCA, RCA+Sand and FA.

Natural rubber latex (NRL) was introduced as an additive to enhance the flexural performance of RCA-based concrete mixtures. The NRL utilized in this study was certified by the Rubber Authority of Thailand, ensuring compliance with industry production standards. The chemical composition of NRL is outlined in **Table 4.2.**

To maintain adequate workability and address low slump values, a water-reducing admixture, specifically Sika® Plastocrete®-907, was incorporated into the concrete mix. This admixture meets the ASTM C494 Type D & G specifications and aids in improving the overall flowability of the concrete.

Table 4.2 Chemical Analysis of Natural Rubber Latex.

Property	Value
Total solid content (TSC)	55.11%
Dry rubber content (DRC)	52.04%
Non rubber contents (NRC)	3.07%
Volatile fatty acid (VFA)	0.07%
Alkalinity (NH_3)	0.69%
pH	10.42%
Mechanical stability time (MST)	7440 s

4.2.2 Specimens Preparation

FA-NRL-RCA concrete specimens were prepared with a fixed water-to-binder ratio (w/b) of 0.4, while varying the dried rubber content-to-binder ratio (r/b). The NRL additive was incorporated at five different percentages relative to the binder (cement + FA) weight e.g. 0%, 0.5%, 1%, 1.5%, and 2.0% to evaluate its influence on workability and water retention in concrete, as referenced by Kim and Robertson (1998), Kim et al. (1999), and Ohama (1998). FA was introduced as a partial cement replacement at three levels: 15%, 20%, and 25% (FA/c). According to **Table 4.2**, the chemical composition of NRL consisted of approximately 52% dry rubber and 48% water. To maintain the designated w/c ratio, adjustments were made to the total mixing water to account for the water content present in the NRL mix.

In this research, NRL was used in liquid form and mixed with distilled water to prepare the concrete specimens. The method followed ensures accurate incorporation of NRL into the mix while maintaining the specified w/b and r/b ratios. Specifically, the distilled water was partially replaced by NRL to achieve the target w/b ratio, as suggested by previous studies (Yaowarat et al., 2021). Considering the NRL contains 52% dry rubber, each kilogram of liquid NRL consists of 520 g of dry rubber and 480 g of water. The required NRL dosage for each r/b ratio was determined using the formula ((r/b)/100)B*(1/0.52), where B represents the total binder content (OPC + FA) in kilograms. To maintain the targeted w/b ratio, the mixing water for the concrete was adjusted using the equation [(w/b)B – 0.48((r/b)/100)B], ensuring that the water introduced through NRL was properly accounted for in the overall mix design.

The mix proportions of the FA-NRL-RCA concretes were meticulously designed following the American Concrete Institute (ACI) methodology, as detailed in **Table 4.3**. RCA was fully utilized as a substitute for natural aggregate, with the fine and coarse aggregate proportions set at 44% and 56%, respectively, adhering to the upper and lower limits prescribed by ASTM C33 (2004). A superplasticizer was incorporated to ensure that the slump values remained within the target range of 40–60 mm for the w/c ratio of 0.4. To mitigate the inherent deficiencies of RCA, such as increased porosity and microcracking caused by the crushing process, the FA-NRL-RCA concrete mixtures were produced using the Two-Stage Mixing Approach (TSMA) as recommended by Tam et al. (2005). This method is specifically employed to enhance RCA quality, ultimately improving the overall mechanical and durability properties of the concrete.

Table 4.3 The mix proportions of the FA-NRL-RCA concretes.

Mix	r/b (wt.)%	OPC (kg/m³)	FA (kg/m³)	Sand (kg/m³)	RCA Coarse Agg. (kg/m³)	Water (kg/m³)	NRL (kg/m³)	SP (kg/m³)	volume (m³)
0%FA	0.0	462.5	0	734	1018	185	0	2.78	0.99008
15%FA	0.0	393.125	69.375	734	1018	185.00	0.00	2.36	0.99708
15%FA+0.5%NRL	0.5	393.125	69.375	734	1018	182.87	4.45	2.36	0.99708
15%FA+1.0%NRL	1.0	393.125	69.375	734	1018	180.73	8.89	2.36	0.99495
15%FA+1.5%NRL	1.5	393.125	69.375	734	1018	178.60	13.34	2.36	0.99281
15%FA+2.0%NRL	2.0	393.125	69.375	734	1018	176.46	17.79	2.36	0.99068
20%FA	0.0	370	92.5	734	1018	185.00	0.00	2.22	0.98855
20%FA+0.5%NRL	0.5	370	92.5	734	1018	182.87	4.45	2.22	0.99942
20%FA+1.0%NRL	1.0	370	92.5	734	1018	180.73	8.89	2.22	0.99942
20%FA+1.5%NRL	1.5	370	92.5	734	1018	178.60	13.34	2.22	0.99728
20%FA+2.0%NRL	2.0	370	92.5	734	1018	176.46	17.79	2.22	0.99515
25%FA	0.0	346.875	115.625	734	1018	185.00	0.00	2.08	0.99301
25%FA+0.5%NRL	0.5	346.875	115.625	734	1018	182.87	4.45	2.08	0.99088
25%FA+1.0%NRL	1.0	346.875	115.625	734	1018	180.73	8.89	2.08	1.00175
25%FA+1.5%NRL	1.5	346.875	115.625	734	1018	178.60	13.34	2.08	1.00175
25%FA+2.0%NRL	2.0	346.875	115.625	734	1018	176.46	17.79	2.08	0.99962

The cement was partially replaced by fly ash (FA) on a mass basis to maintain consistency with the reference RCA–NRL concrete used for comparison. Although mass-based replacement can introduce slight volumetric variation due to the lower specific gravity of FA, the mix proportions were carefully adjusted to ensure a total volume of approximately 1.00 m^3 for all mixtures, as shown in **Table 4.3**. This approach allows a direct evaluation of FA's influence on hydration behavior, microstructural refinement, and long-term performance while maintaining comparable batch volumes. A total binder content of approximately 450 kg/m³ was adopted for the mix design to meet the requirements of rigid pavement applications in accordance with the Department of Highways, Thailand specification (DH-S309/2544), which specifies minimum strengths of fc ≥ 32 MPa and ff ≥ 4.2 MPa at 28 days. This relatively high binder content was selected to ensure adequate fatigue resistance and workability for pavement-grade concrete while compensating for the higher porosity and water absorption of RCA.

4.2.3 Engineering and Microstructural Investigation

4.2.3.1 Compressive strength (f_c) and flexural strength (f_f)

The FA-RCA-NRL concrete specimens were prepared following the ACI method, aiming to achieve a f_c of 350 ksc (34.3 MPa) at w/c = 0.4, as presented in **Table 4.3**. A rotary drum mixer was employed to ensure uniform distribution of all components throughout the mixing process. The workability of the fresh concrete mixture was assessed using the slump test, conducted in accordance with ASTM C143 (2015). To evaluate the f_c, cubic concrete specimens measuring 150 x 150 x 150 mm^3 were cast following the standards outlined in BS 1881 Part 3 (1983). Similarly, for f_f, testing beam-shaped specimens of 100 x 100 x 400 mm^3 were prepared. The fresh FA-RCA-NRL concrete was poured into molds in three layers, with each layer compacted using a 4-pound steel ram, applying 35 strokes per layer, as specified in ASTM C192 (2019). The specimens were cured in a moist environment at a controlled temperature of 27^o – 29^o to ensure proper hydration and strength development. After 7, 28 and 56 days, f_c testing was performed following either BS 1881 Part 4 (1983) or ASTM C39 (2021) standards. For f_f evaluation, the beam specimens underwent a third-point loading test, where two loads were applied to divide the beam span into three equal sections, adhering to ASTM C78 (2021). The f_f values of the FA-RCA-NRL concretes were subsequently calculated using the relevant equation based on these experimental procedures.

$$\text{Flexural strength } (f_f) = \frac{PL}{bd^2} \tag{4.1}$$

where P is the maximum load, L is the span length, and b and d are the average width and depth of the specimen.

The average values of f_c and f_f were determined based on data obtained from three test specimens. To ensure the reliability and consistency of the results, these values were rigorously evaluated within the standard deviation (SD) threshold, following the criterion SD/□ < 10%, where □ represents the mean value of either f_f or f_c.

4.2.3.2 Flexural Fatigue

The three-point flexural fatigue test was conducted on FA-RCA-NRL concrete specimens, maintaining the same mix proportions and dimensions as those used in flexural strength testing. A 500 kN electro-hydraulic servo testing machine equipped with an autonomous data recorder was utilized to evaluate fatigue performance. The impact of NRL and FA incorporation on the fatigue resistance of concrete beams was evaluated across all r/b and FA replacement ratios by applying cyclic vertical loads at stress ratio (SR) levels of 60%, 70%, and 80%, referenced to their flexural strength (f_f). To ensure a consistent loading condition throughout the test, a stress-controlled approach was implemented to maintain a constant load at the target SR.

The stress ratio (SR), which accounts for both applied flexural stress and concrete strength, was determined using the equation proposed by Smith and Roesler (2004)

$$SR = \frac{\sigma}{f_f} \tag{4.2}$$

where σ represents the applied flexural stress, and f_f denotes the flexural strength of the FA-RCA-NRL concrete.

To simulate the vehicular traffic loading conditions expected in pavement applications, a haversine loading pulse with a frequency of 10 Hz was applied to the FA-RCA-NRL concrete specimens.

To improve the reliability and transparency of the experimental findings, all bar charts illustrating compressive strength, flexural strength, and fatigue life were updated to include error bars representing one standard deviation (SD), derived from three specimens per mix condition. This addition highlights the reproducibility of the results and provides a clearer visualization of data variability across the tested mixtures.

4.2.3.3 Scanning electron microscopy (SEM) and Energy-Dispersive X-ray spectroscopy (EDX)

The development of f_c and f_f in relation to varying r/b and FA replacement ratios was analyzed using scanning electron microscopy (SEM), energy-dispersive X-ray spectroscopy (EDX). To facilitate SEM and EDX examinations, a thin section of the specimen was first frozen at -195°C in liquid nitrogen and subsequently coated with a protective gold layer, ensuring optimal image quality for SEM analysis (Yaowarat et al. 2018).

4.2.3.4 Calculation of carbon emissions

Life cycle assessment is a cradle-to-grave or cradle-to-cradle analysis technique to assess environmental impacts associated with all the stages of a product's life, which is from raw material extraction through materials processing, manufacture, distribution, and use. The carbon is a dominant category to assess the environment impacts compared to other impact categories (Lazarevic and Martin 2016; Reijnders 2012). The carbon footprint is a key greenhouse gas that drives global climate change and global warming effect (Hertwich and Peters 2009). In practice, the evaluation of carbon footprint of a product is the key process for the life cycle assessment. Carbon emissions was calculated using the following equation:

$$\sum CO_2 = V \times EF \quad (4.3)$$

where *V* is the amount of tested materials (kg), and *EF* is the emission factors of tested materials (kg CO_2-e/kg).

4.3 RESULTS

4.3.1 Compressive strength of FA-RCA-NRL concrete

Figure 4.2 illustrates the compressive strength (f_c) development of FA-RCA-NRL concrete specimens cured for 7, 28, and 56 days, with FA replacement levels of 0% (Youromphruk et al. 2025), 15%, 20%, and 25%, and various r/b ranging from 0.0% to 2.0%, under a constant w/b ratio of 0.4. At all curing periods, the specimens without NRL (r/b = 0%) exhibited the highest f_c. As expected, the f_c of all mixtures increased with longer curing durations, while it decreased with an increasing r/b ratio. For instance, at 7 days (**Figure 4.2(a)**), the f_c of the control mix (r/b = 0%) reached 42.80 MPa for FA = 0% (Youromphruk et al. 2025), which was higher than the corresponding values of 41.14 MPa, 38.32 MPa, and 37.52 MPa for FA replacement levels of 15%, 20%, and 25%, respectively. However, when the r/b ratio was increased to 2.0%, the f_c values dropped markedly to 25.80 MPa for FA = 0% and to 25.68 MPa, 24.44 MPa, and 23.32 MPa for FA = 15%, 20%, and 25%, respectively. A similar trend was observed at 28 days (**Figure 4.2(b)**), where the control mixes continued to outperform the NRL-modified ones. The f_c values at r/b = 0% were 49.10 MPa for FA = 0% (Youromphruk et al. 2025), followed by 48.52 MPa, 46.47 MPa, and 45.15 MPa for FA levels of 15%, 20%, and 25%, respectively. In contrast, at the highest NRL content (r/b = 2.0%), the f_c values decreased to 31.00 MPa for FA = 0% and to 28.92 MPa, 28.43 MPa, and 27.57 MPa for FA = 15%, 20%, and 25%, respectively.

Interestingly, the 56-day strength results (**Figure 4.2(c)**) reveal a noteworthy gain in f_c, particularly for higher FA replacement levels. For example, the control mix (r/b = 0%) demonstrated increasing strength with increasing FA content, reaching 53.35 MPa, 55.78 MPa, and 59.63 MPa for 15%, 20%, and 25% FA, respectively. This long-term strength gain is attributed to the pozzolanic reaction of FA, which becomes more pronounced over time. Despite the strength reductions observed at early ages with higher r/b ratios, the 56-day strength results for NRL-modified mixes showed measurable improvement. At r/b = 2.0%, f_c improved to 33.10 MPa, 33.76 MPa, and 32.76 MPa for FA contents of 15%, 20%, and 25%, respectively indicating that the delayed strength development associated with NRL and FA can be partially recovered over time.

The horizontal dotted line in **Figure 4.2(b)** indicates the minimum f_c requirement for rigid pavement, as specified by the Department of Highways, Thailand (f_c > 32 MPa at 28-day) [DH-S309/2544]. It was observed that the control mixtures without NRL (r/b = 0%) met the requirement for all levels of FA replacement. In particular, the FA = 0% mix achieved the highest compressive strength at 28 days (49.1 MPa), clearly surpassing the minimum requirement and outperforming the FA-blended concretes. For mixes incorporating NRL, the requirement was still satisfied at r/b ≤ 1.0%

for FA = 15% and FA = 20%, with f_c of 41.21 MPa and 36.63 MPa at r/b = 0.5%, and 37.63 MPa and 32.78 MPa at r/b = 1.0%, respectively. However, for FA = 25%, only the mixes with r/b = 0.5% (35.28 MPa) met the standard. Mixes with r/b ≥ 1.5% for all FA replacement levels fell below the required 32 MPa threshold, highlighting that higher NRL content adversely affected strength development at 28 days. This suggests that, for applications requiring compliance with the Department's rigid pavement criteria, the allowable r/b ratio should be limited according to the FA content: up to 1.0% for FA levels below 20%, and restricted to 0.5% when FA content reaches 25%.

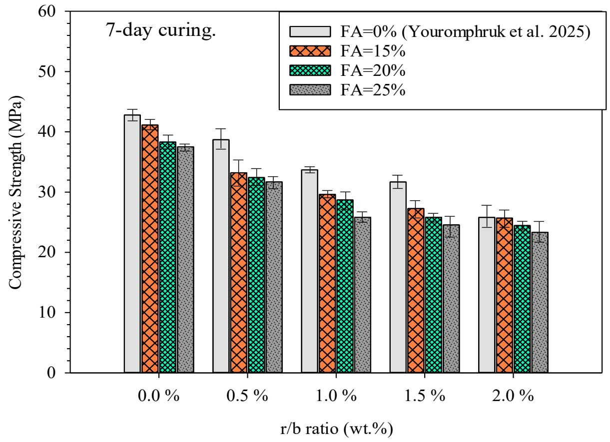

(a)

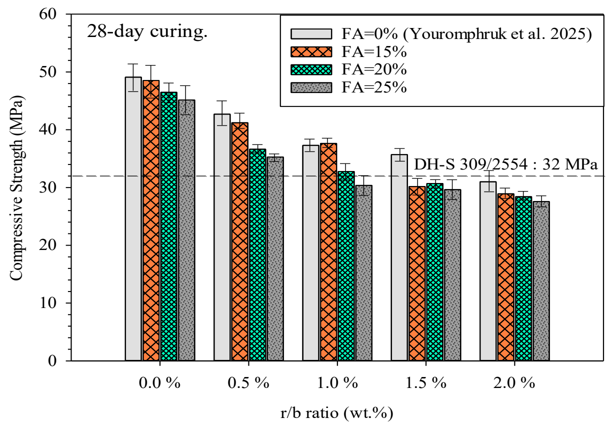

(b)

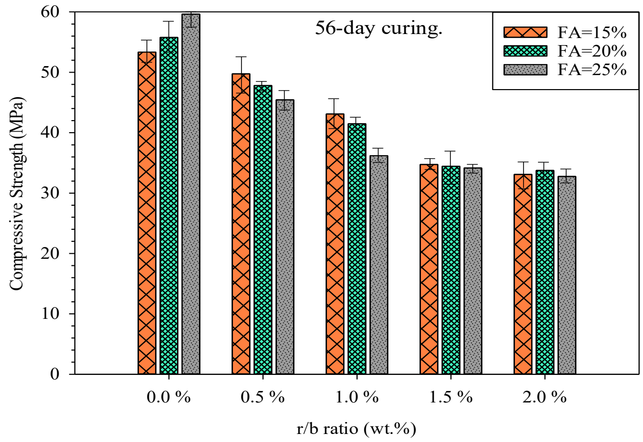

(c)

Figure 4.2 Compressive strength of FA-RCA-NRL concrete at (a) 7 days; (b) 28 days; (c) 56 days.

4.3.2 Flexural strength of FA-RCA-NRL concrete

Figure 4.3 presents the f_f development of FA-RCA-NRL concrete specimens at 7, 28, and 56 days with different FA replacement levels (0%, 15%, 20%, and 25%) and r/b ratios of 0.0%, 0.5%, 1.0%, 1.5%, and 2.0%, under a constant w/b ratio of 0.4. The results indicated that at a given r/b ratio and FA content, f_f increased over time, with the highest values observed at 56 days, similar to the compressive strength trend. At 7 days (**Figure 4.3(a)**), the control mix (r/b = 0%) exhibited the highest f_f, reaching 4.15 MPa for FA = 0% (Youromphruk et al. 2025), which was slightly higher than the values of 4.00 MPa, 3.80 MPa, and 3.66 MPa for FA levels of 15%, 20%, and 25%, respectively. With the incorporation of NRL, the f_f decreased across all FA contents, particularly at r/b ≥ 1.5, where the f_f values dropped to 3.55 MPa for FA = 0% (Youromphruk et al. 2025) and to 3.26 MPa, 3.22 MPa, and 2.75 MPa for FA = 15%, 20%, and 25%, respectively.

At 28 days (**Figure 4.3(b)**), an increase in f_f was observed across all mixes. The control concrete (r/b = 0%) achieved 4.65 MPa for FA = 0% (Youromphruk et al. 2025), compared with 4.55 MPa, 4.50 MPa, and 3.92 MPa for FA replacement levels of 15%, 20%, and 25%, respectively. The highest f_f was recorded at r/b = 0.5, where f_f exceeded that of the control mix, reaching 4.82 MPa for FA = 0% (Youromphruk et al. 2025) and 4.57 MPa, 4.62 MPa, and 4.38 MPa for FA = 15%, 20%, and 25%, respectively.

At r/b = 1.0, a slight reduction was noted, with corresponding values of 4.62 MPa for FA = 0% (Youromphruk et al. 2025) and at 4.68 MPa, 4.57 MPa and 3.76 MPa for FA = 15%, 20% and 25%, respectively. Beyond this level, a consistent decline in f_f was evident, with r/b = 2.0 producing the lowest values: 3.72 MPa for FA = 0% (Youromphruk et al. 2025) and to 3.69 MPa, 3.16 MPa, and 2.89 MPa for FA = 15%, 20%, and 25%, respectively. These results suggest that a low-to-moderate NRL dosage (r/b = 0.5-1.0%) enhances flexural performance, whereas higher dosages (r/b ≥ 1.5%) negatively affect strength development, likely due to changes in the cementitious matrix and bond structure.

At 56 days (**Figure 4.3(c)**), the highest f_f was recorded, with f_f exceeding 5.0 MPa for some mixes. The control mix (r/b = 0%) exhibited 4.82 MPa, 4.92 MPa, and 5.47 MPa for FA replacement levels of 15%, 20%, and 25%, respectively. The highest recorded f_f was 5.62 MPa at r/b = 0.5% and FA = 25%, suggesting that a moderate addition of NRL contributed positively to long-term strength development. However, a decline was noted for r/b ≥ 1.5, where f_f values dropped to 4.13 MPa, 4.54 MPa, and 3.56 MPa at FA levels of 15%, 20%, and 25%, respectively.

The f_f of FA-RCA-NRL concrete exhibited ages-dependent trends rather than a single distinct pattern. At 7 days, f_f generally decreased with increasing r/b ratio for all FA levels, which is attributed to the insufficiently developed cementitious matrix at early age; consequently, NRL is not yet effective and higher latex contents can even disrupt hydration. At 28 days, an optimum emerged: mixes with r/b ≈ 0.5–1.0% achieved equal or higher f_f than the r/b = 0% control for FA = 15–20% (with the peak at r/b = 1.0%), while the FA = 25% series benefited only at r/b = 0.5% and declined beyond this dosage. By 56 days, the optimum shifted toward r/b ≈ 0.5% for all FA levels, after which f_f decreased markedly at higher r/b ratios of ≥1.5%. This evolution reflects the combined effects of latex-film coalescence and the delayed pozzolanic reaction of FA, which enhance matrix integrity at moderate NRL dosages.

The horizontal dotted line in **Figure 4.3(b)** represents the minimum f_f requirement for rigid pavements, as per the Department of Highways, Thailand (f_f > 4.2 MPa at 28-day) [DH-S309/2544]. The control concrete (r/b = 0%) met this requirement for FA = 0%, 15% and 20% at 28 days but failed for FA = 25%. Among the NRL-modified concretes, the requirement was satisfied for r/b ≤ 1.0% at FA = 0%, 15% and 20%, achieving f_f above 4.2 MPa. For FA = 25%, only the mix with r/b = 0.5% met the standard, recording 4.38 MPa at 28 days, while r/b ≥ 1.5% failed to meet the requirement across all FA levels. When evaluating both f_c and f_f requirements, the control concrete (r/b = 0%) met the requirement when FA < 20%, while FA-RCA-NRL-concrete met the requirement when r/b ≤ 1.0% for FA < 20%, and when r/b = 0.5% for FA < 25%. These findings suggest that while NRL improves workability and water retention, its proportion must be optimized to ensure compliance with structural performance standards. Moreover, the inclusion of FA contributes long-term benefits through its pozzolanic reaction, which improves the microstructure, enhances durability, and supports continued strength development beyond 28 days, thereby improving the overall service life of RCA-based pavement concrete.

4.3.3 Fatigue performance

Figure 4.4 illustrates the fatigue performance of FA-RCA-NRL concrete at 28 days of curing, incorporating various levels of FA replacement (15%, 20%, and 25%) and r/b, under three applied stress ratios (60%, 70%, and 80%). It should be noted that the fatigue behavior of the FA = 0% mixtures was not further investigated in this study, since the research objective focused on reducing cement consumption to lower material costs and mitigate greenhouse gas emissions. In addition, the results of compressive and flexural strength tests confirmed that concretes with FA replacement levels of 15–25% still satisfied the minimum requirements of the Department of Highways, Thailand with superior long-term performance, ensuring their suitability for pavement applications.

In general, fatigue life decreased as the stress ratio increased, regardless of FA content or r/b ratio. For example, at FA = 15% (**Figure 4.4(a)**), the fatigue life of unmodified concrete (r/b = 0%) was 2022, 750, and 122 cycles at stress ratios of 60%, 70%, and 80%, respectively. The inclusion of NRL at r/b = 0.5% significantly enhanced the fatigue life to 2564, 895, and 263 cycles under the same stress levels. However, increasing the r/b ratio beyond 1.0% resulted in a gradual reduction in fatigue life, reaching the lowest values of 1507, 562, and 55 cycles at r/b = 2.0%, likely due to excessive NRL content retarding hydration and limiting pozzolanic reaction.

A similar trend was observed at FA = 20% (**Figure 4.4(b)**), where the fatigue life of the unmodified mix (r/b = 0%) was 2546, 988, and 253 cycles at 60%, 70%, and 80% stress ratios, respectively. The optimum fatigue performance was again recorded at r/b = 0.5%, where fatigue life increased to 2868, 1263, and 364 cycles, demonstrating that moderate NRL content improves resistance to cyclic loading. Beyond this point, further increases in r/b caused a decline in fatigue life, with the lowest values at r/b = 2.0% being 1954, 659, and 126 cycles, similar to the pattern found with 15% FA. At FA = 25% (**Figure 4.4(c)**), all mixes exhibited generally lower fatigue life compared to those with 15% and 20% FA replacement ratios. The unmodified mix (r/b = 0%) recorded fatigue lives of 2269, 785, and 62 cycles at the respective stress ratios. As with the other FA levels, the addition of NRL at r/b = 0.5% improved performance to 2436, 863, and 87 cycles. However, as the r/b ratio increased further, fatigue life diminished, with r/b = 2.0% yielding the lowest recorded values of 1544, 201, and 39 cycles.

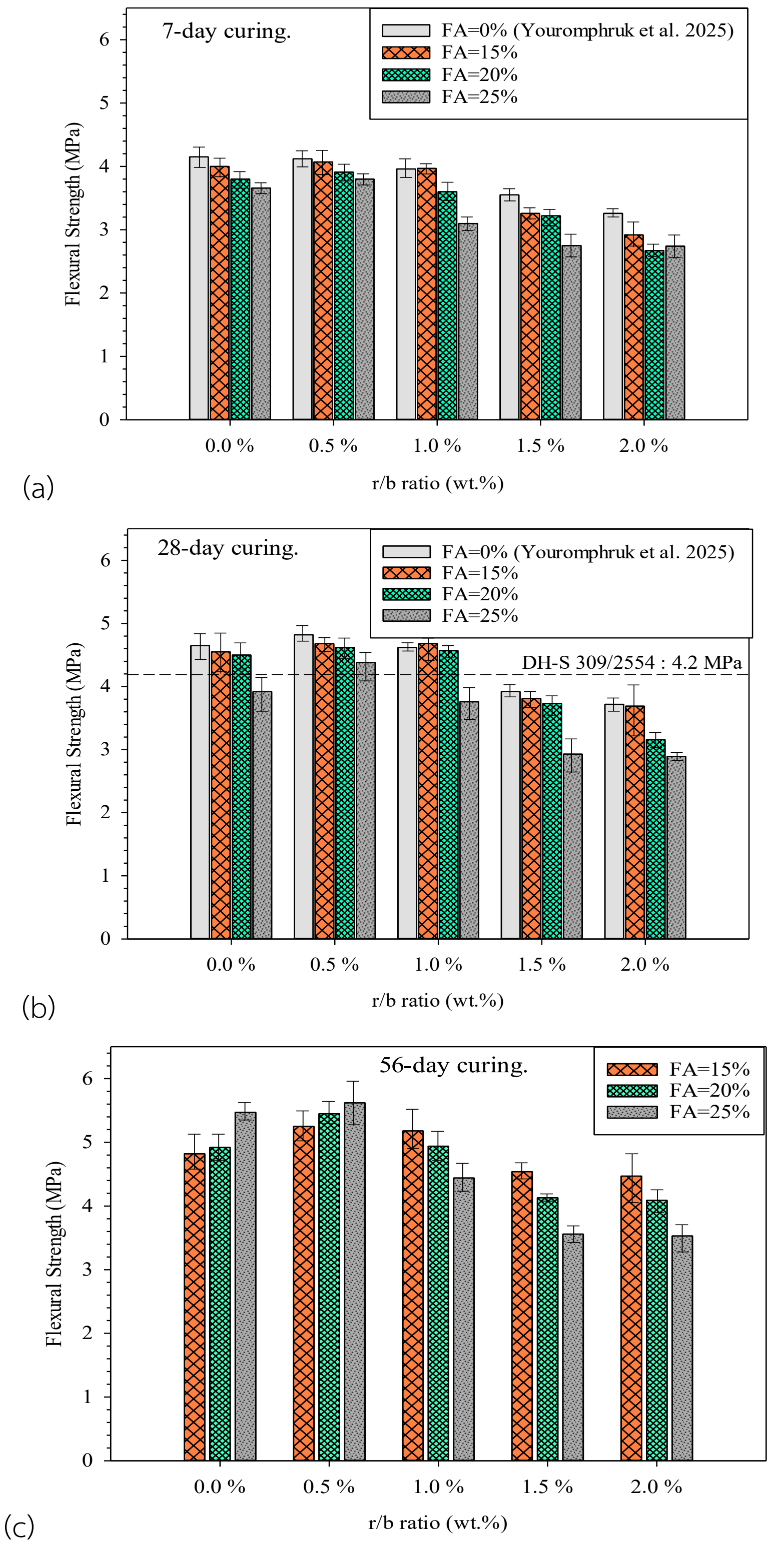

Figure 4.3 Flexural strength of FA-RCA-NRL concrete at (a) 7 days; (b) 28 days; (c) 56 days.

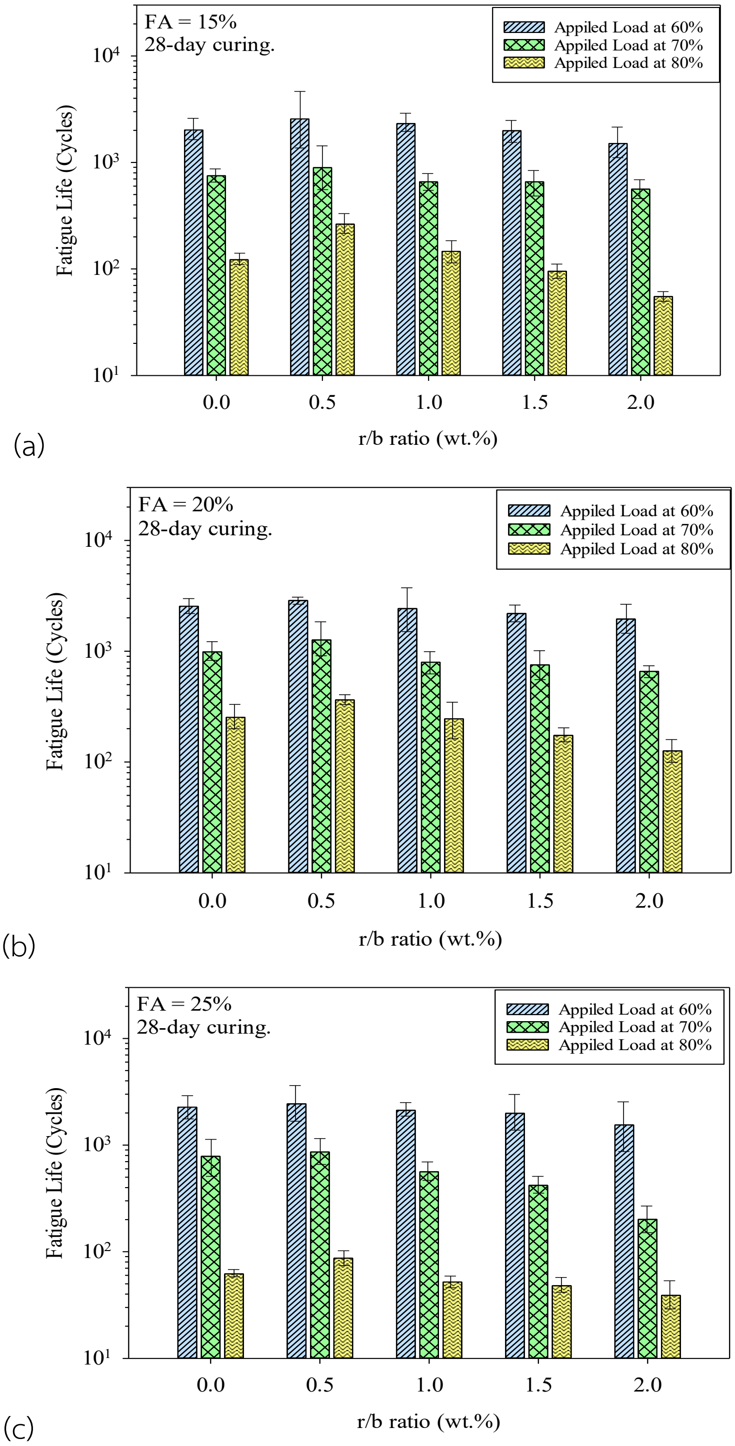

Figure 4.4 Fatigue life of FA-RCA-NRL concrete at 28 days for FA replacement levels of (a) 15%, (b) 20%, and (c) 25%.

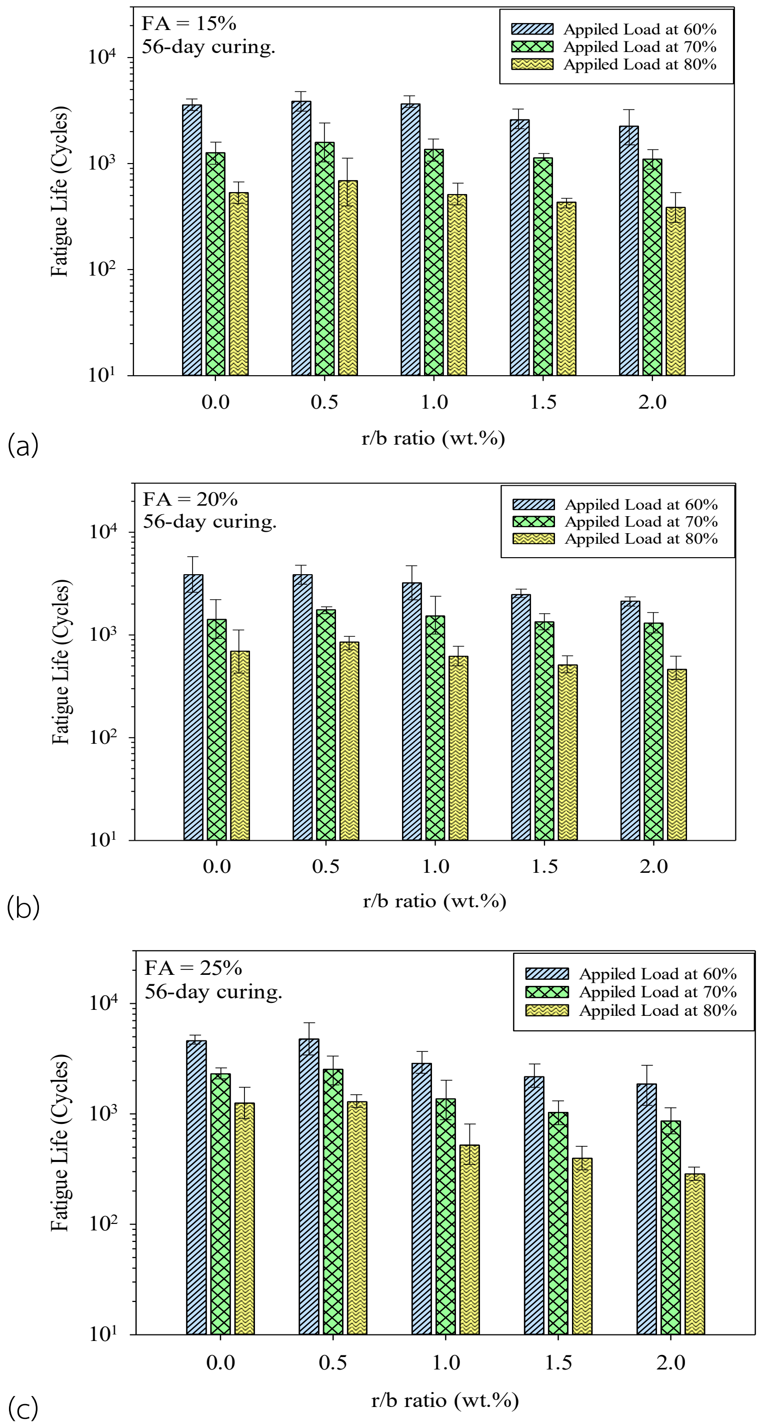

Figure 4.5 Fatigue life of FA-RCA-NRL concrete at 56 days for FA replacement levels of (a) 15%, (b) 20%, and (c) 25%.

Figure 4.5 illustrates the fatigue performance of FA-RCA-NRL concrete at 56 days of curing, incorporating various levels of FA replacement (15%, 20%, and 25%) and different r/b ratios, under three applied stress ratios (60%, 70%, and 80%). At 15% FA replacement ratio (**Figure 4.5(a)**), the unmodified concrete (r/b = 0%) exhibited moderate fatigue resistance, recording 3567, 1265, and 532 cycles at stress ratios of 60%, 70%, and 80%, respectively. These values reflect limited long-term performance, particularly under high-stress conditions, likely due to the relatively low pozzolanic reactivity at this replacement level. Importantly, the incorporation of NRL at an optimum dosage (r/b = 0.5) extended the fatigue life to 3856, 1584 and 689 cycles at stress ratios of 60%, 70%, and 80%, respectively, confirming the beneficial interaction of latex film formation and FA-induced microstructural refinement at later ages. However, when the r/b ratio increased to 2.0, the fatigue life significantly decreased to 2247, 1101, and 386 cycles, suggesting that excessive NRL content impaired hydration and weakened bonding within the cementitious matrix.

At 20% FA replacement (**Figure 4.5(b)**), the unmodified concrete (r/b = 0%) showed a marked improvement, achieving 3862, 1416, and 696 cycles at the respective stress levels. In this case, the addition of NRL at r/b = 0.5 further enhanced fatigue performance to 3896, 1756 and 852 cycles at stress ratios of 60%, 70%, and 80%, respectively, particularly under low-to-moderate stress ratios, highlighting the synergistic effect of FA’s pozzolanic activity and latex bridging in prolonging fatigue life. Although a reduction in fatigue life was observed at r/b = 2.0%, with values of 2136, 1306, and 463 cycles, the overall performance remained acceptable—especially under lower and moderate stress ratios. This indicates that the higher pozzolanic activity at 20% FA helped mitigate the negative effects of elevated NRL dosage.

The trend continued at 25% FA (**Figure 4.5(c)**), where the unmodified concrete (r/b = 0%) achieved the highest fatigue life among all tested groups: 4596, 2305, and 1253 cycles at 60%, 70%, and 80% stress ratios, respectively. At this FA level, the presence of NRL at r/b = 0.5 sustained high fatigue resistance even beyond the control mix, with values of 4768, 2534, and 1288 cycles, underscoring the strong synergy between high-volume FA and moderate latex addition. Notably, even at r/b = 2.0, the fatigue performance remained relatively robust, with 1863, 862, and 286 cycles.

Although this represented a reduction compared to the unmodified mix, the decline was more gradual, suggesting that high-volume FA contributes to improved matrix resilience and can partially offset the detrimental impact of excessive latex content. Overall, these findings emphasize the critical role of FA replacement level in moderating the influence of NRL on fatigue life, especially over extended curing periods. In addition to fatigue life, **Figure 4.6** illustrates the displacement response of FA-RCA-NRL concrete under flexural fatigue loading at a stress ratio of 60%, incorporating 25% FA replacement and a constant w/c ratio of 0.4 across various r/b ratios. The number of cycles to failure (Nf) is plotted along the x-axis, while the y-axis represents the total displacement at the center of the beam during cyclic loading. The unmodified concrete (r/b = 0%) exhibited moderate fatigue life, with a notable increase in displacement toward the final stages of loading, indicating failure after about 80% of its fatigue life. In contrast, the mix with r/b = 0.5% showed the highest fatigue life and noticeably lower displacement accumulation than the mixes with r/b = 1.5%, and 2.0%, identifying it as the optimum r/b ratio for this mix. This trend is consistent with the findings of Suddeepong et al. (2022), which demonstrated that low dosages of NRL can enhance ductility, energy absorption, and fatigue resistance by improving the microstructural bond and limiting microcrack propagation. However, further increases in r/b ratio to 1.0, 1.5, and 2.0 led to a noticeable decline in fatigue performance, as seen in the lower fatigue life and greater displacement accumulation. This behavior is attributed to the adverse effects of excessive latex, which can retard hydration, disrupt matrix formation, and increase plastic deformation. The shape of the displacement curves also reflects the typical three-phase fatigue behavior observed in cementitious materials: an initial phase of crack initiation, a stable crack propagation phase, and a final phase characterized by rapid displacement growth leading to failure. The r/b = 0.5 mix maintained a prolonged stable phase with low deformation progression, suggesting superior crack control and energy dissipation under repeated loading.

Figure 4.7 presents the flexural fatigue performance of FA-RCA-NRL concrete at 56 days of curing under stress ratios of 60%, 70%, and 80%, with varying r/b ratios and FA replacement levels of 15%, 20%, and 25%, compared with the PCA (1984) fatigue model. The results show that the NRL-modified RCA concretes scatter closely around the PCA model line, confirming that SR predominantly governs fatigue life. The results clearly showed that fatigue life was strongly influenced by both the r/b ratio and the applied stress ratio. At FA = 15%, the unmodified mix (r/b = 0%) recorded fatigue lives of 3567, 1265, and 532 cycles at stress ratios of 60%, 70%, and 80%, respectively. A similar trend was observed at FA = 20%, where the unmodified mix achieved 3862, 1416, and 696 cycles. The peak performance was again at r/b = 0.5% (3996, 1756, and 852 cycles), suggesting an optimum NRL dosage. Beyond this point, fatigue life progressively declined, particularly at r/b = 2.0%, where the fatigue life dropped to 2136, 1306, and 463 cycles. These findings align with (Suddeepong et al. 2022), who demonstrated that NRL-modified concrete at optimum r/b ratios exhibits superior flexural fatigue resistance compared with conventional concrete, due to reduced plastic deformation and improved ductility.

Figure 4.7 presents the regression analysis between the logarithmic fatigue life (log Nf) and the applied stress ratio (SR) for the FA–NRL–RCA concrete. This behavior demonstrates the beneficial effect of optimal NRL incorporation in improving the fatigue resistance of FA–RCA concrete. The strong correlation between the measured and predicted fatigue lives further confirms that the proposed regression model reliably represents the fatigue behavior of the developed mixtures.

From a mechanistic design perspective, the Department of Highways (DH-S309/2544) specifies fatigue life as a controlling factor in rigid pavement performance. For normal concretes, fatigue life is strongly governed by the stress ratio (SR) in accordance with the PCA model. However, recent studies indicate that in NRL-concretes, this relationship is modified: at equivalent SR, the presence of latex films improves crack resistance and extend fatigue life beyond conventional predictions. This suggests that mix design for NRL-concrete pavement should not only satisfy compressive (f_c > 32 MPa) and flexural strength (f_f > 4.2 MPa) requirements but also optimize the r/b ratio at ~0.5 to achieve superior fatigue performance. By adopting this approach, pavement thickness can potentially be reduced without compromising service life, offering both economic and sustainability benefits, consistent with design recommendations by (Suddeepong et al. 2022 and Yaowarat et al. 2021).

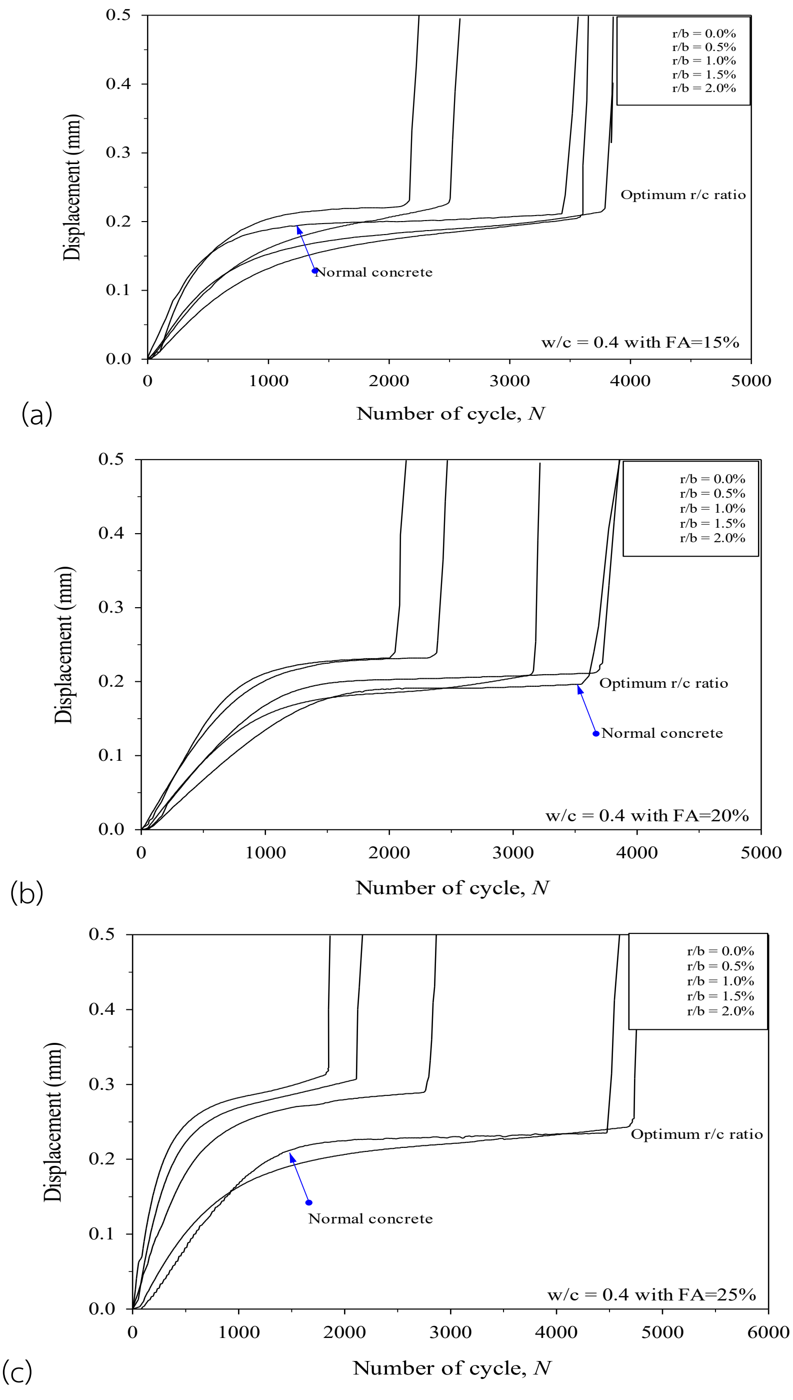

Figure 4.6 Flexural fatigue response of FA-RCA-NRL concrete under a stress ratio of 60% after 56 days for FA replacement levels of (a) 15%, (b) 20%, and (c) 25%.

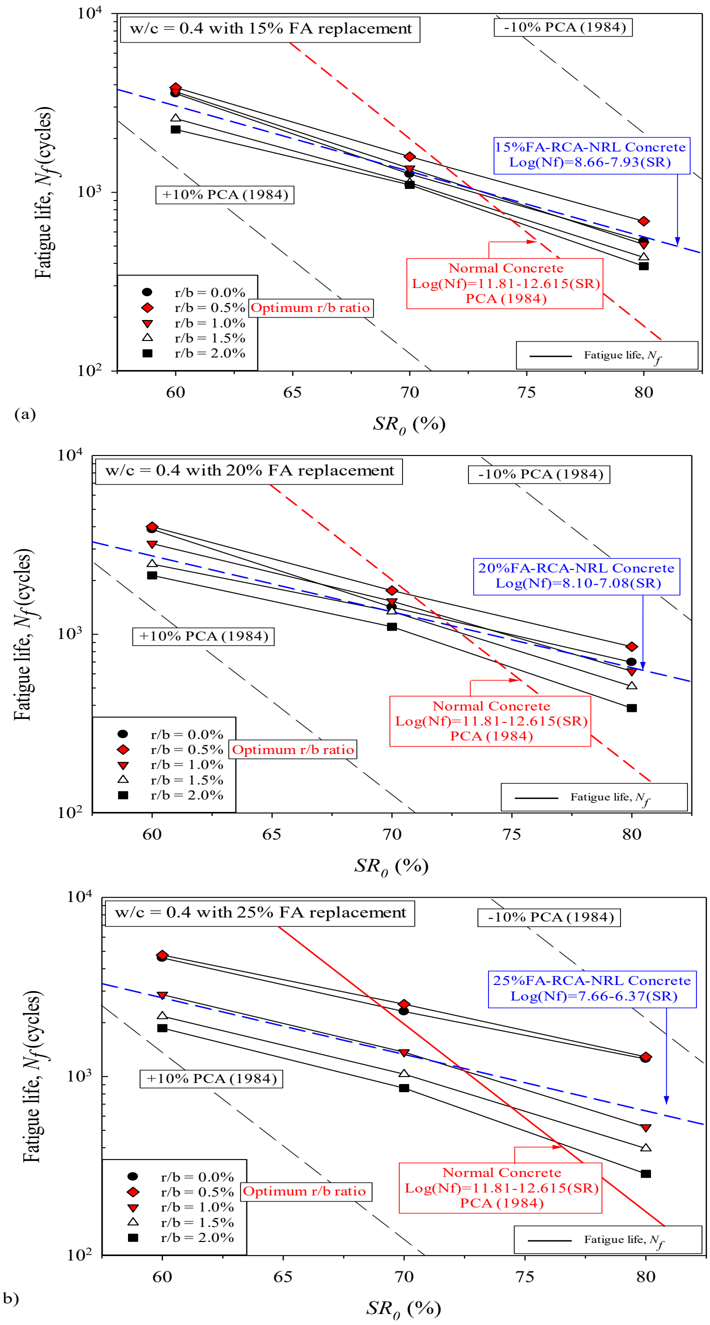

Figure 4.7 Effect of r/b ratio on fatigue life versus SR_0 relationship of FA-RCA-NRL concrete at 56 days for varying fly ash replacement levels: (a) 15%, (b) 20%, and (c) 25%.

4.4 MICROSTRUCTURAL ANALYSIS

To understand the microstructural characteristics of FA-RCA-NRL concrete, scanning electron microscope (SEM) analysis was performed at 28 days of curing. The SEM was operated at 15 kV with secondary electron imaging to characterize the morphology of the concrete surface. **Figure 4.8** illustrates the microstructure of FA-RCA-NRL concrete incorporating 25% FA as a partial cement replacement and varying r/b ratios of 0%, 0.5%, and 2%. In **Figure 4.8(a)** (r/b = 0%), the microstructure displays a relatively dense matrix with well-formed C-S-H gel and needle-like ettringite crystals, reflecting active early-age hydration (Park et al. 2016; Yaowarat et al. 2019). Smooth and spherical FA particles are embedded in the matrix, indicating partial pozzolanic reaction (Arulrajah et al. 2019; Elyasigorji et al. 2023; Golewski 2022). In the absence of NRL, no polymer films are observed, allowing for uninterrupted hydration and gel formation. In **Figure 4.8(b)**, corresponding to the optimal r/b ratio of 0.5%, the microstructure appears more homogeneous and compact compared to the r/b = 0% mix **(Figure 4.8(a))**. Thin and continuous NRL films were evident, interwoven with the hydration products and bridging microvoids within the matrix. These films likely fill capillary pores and reinforce interfacial zones, resulting in enhanced flexural strength and fatigue life due to the improved ductility and crack-bridging capability of the latex (Hoy et al. 2023; Li et al. 2021; Stirewalt 2021). The smoother surface texture and denser C-S-H gel formation suggest a favorable interaction between pozzolanic FA reaction and moderate latex addition. The microstructure at this dosage reflects a balanced synergy: sufficient hydration, strong inter-particle bonding, and enhanced toughness from the polymer network (Yaowarat et al. 2018; Yaowarat et al. 2021).

In contrast, **Figure 4.8(c)**, representing a higher r/b ratio of 2%, shows a more porous and disrupted morphology. Thicker NRL films are visible, particularly around unreacted or partially hydrated FA particles and hydration products. These films appear to cluster or isolate phases, forming physical barriers that retard water transport and ion exchange, which are essential for continued hydration (Han et al. 2024; Kang et al. 2015; Knapen and Van Gemert 2015; Wang et al. 2023). The resulting structure is less cohesive, with poorly developed C-S-H gel and visible voids. This morphology correlates with a reduction in compressive strength, as the excessive latex interferes with the formation of continuous cementitious bonds. Moreover, the plastic nature of the excess NRL may have introduced internal weaknesses that compromise the material's load-bearing capacity under compression (Awoyera et al. 2024).

In **Figure 4.9(a)** (r/b = 0%), the matrix revealed a dense and well-developed microstructure, featuring numerous etched spherical FA particles and needle-like ettringite crystals embedded within a continuous C-S-H gel network. The pronounced surface dissolution of the FA indicates active and advanced pozzolanic reaction, contributing to the formation of additional cementitious products (Golewski 2022; Kang et al. 2022; Wang and Ishida 2019). Although some voids remain due to the absence of NRL, the unimpeded hydration enables the development of a cohesive and well-bonded matrix. This results in the highest compressive strengths among the mixes, as the structure benefits from complete gel formation without interference from polymer films.

Figure 4.9(b) (r/b = 0.5%) represents the optimal latex dosage, showing a compact and refined microstructure. The matrix is densely packed with granular C-S-H and well-integrated FA particles. The inset magnification reveals thin NRL films bridging microvoids and bonding hydration products, which improve flexural performance through crack-bridging effects. While some porosity persists, the synergistic effect of FA and moderate latex dosage fosters both pozzolanic reactivity and matrix reinforcement. The structure is optimized for bending resistance, explaining its superior flexural strength at this dosage. In **Figure 4.9(c)** (r/b = 2%), the matrix deteriorates visibly. The microstructure is porous, with disconnected gel phases and clusters of unreacted or partially reacted FA particles. Thick, continuous latex films dominate the surface, forming barriers around hydration sites. These films restrict water movement and reduce the efficiency of hydration and pozzolanic reactions, leading to a fragmented and weakly bonded matrix (Naseem et al. 2023; Yaowarat et al. 2021). The excess polymer acts more as an insulator than a reinforcing agent, correlating with the lowest compressive strength among the mixes.

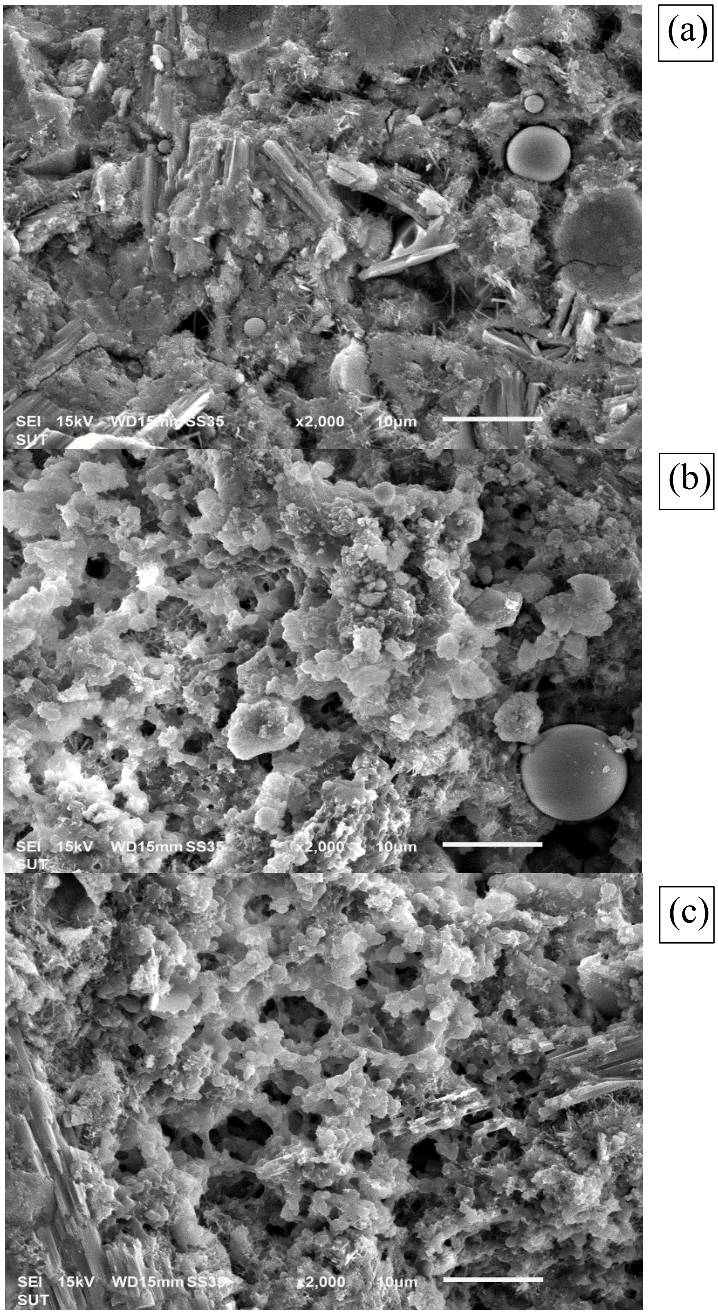

Figure 4.8 SEM images of FA-RCA-NRL concrete at 28 days with 25% fly ash replacement and r/b ratios of (a) 0%, (b) 0.5% (optimal), and (c) 2%

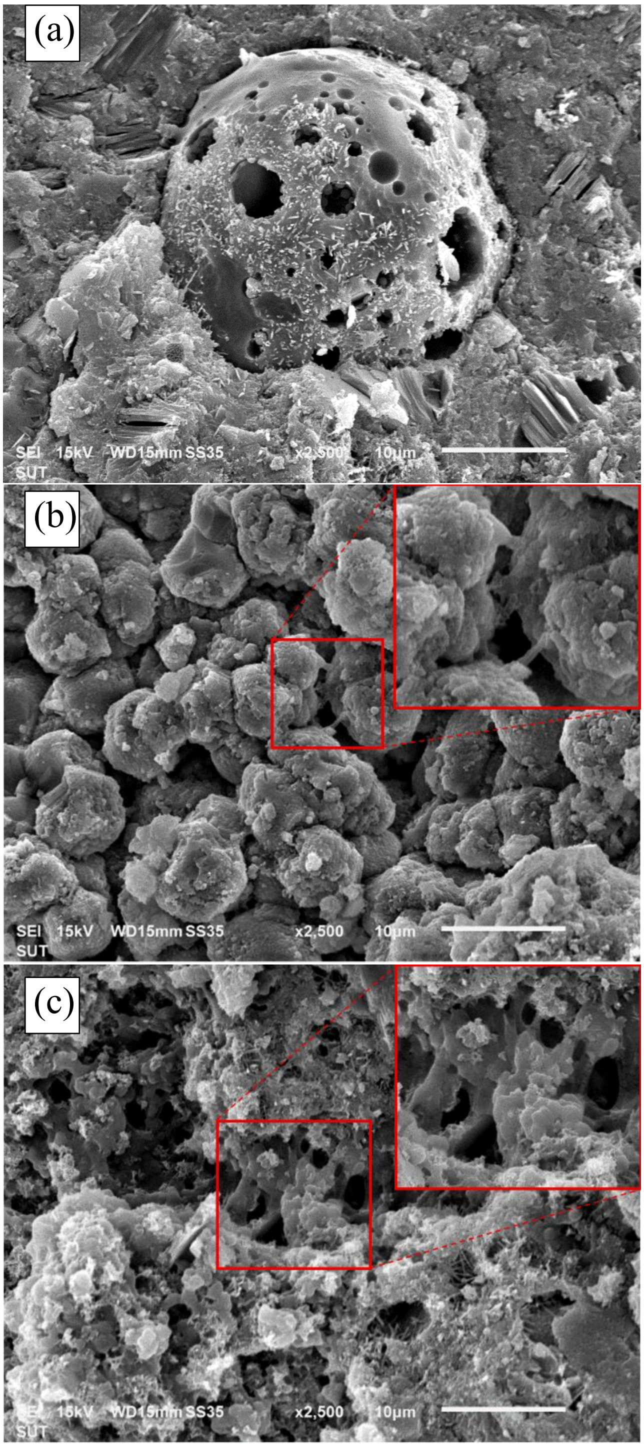

Figure 4.9 SEM images of FA-RCA-NRL concrete at 56 days with 25% fly ash replacement and r/b ratios of (a) 0%, (b) 0.5% (optimal), and (c) 2%

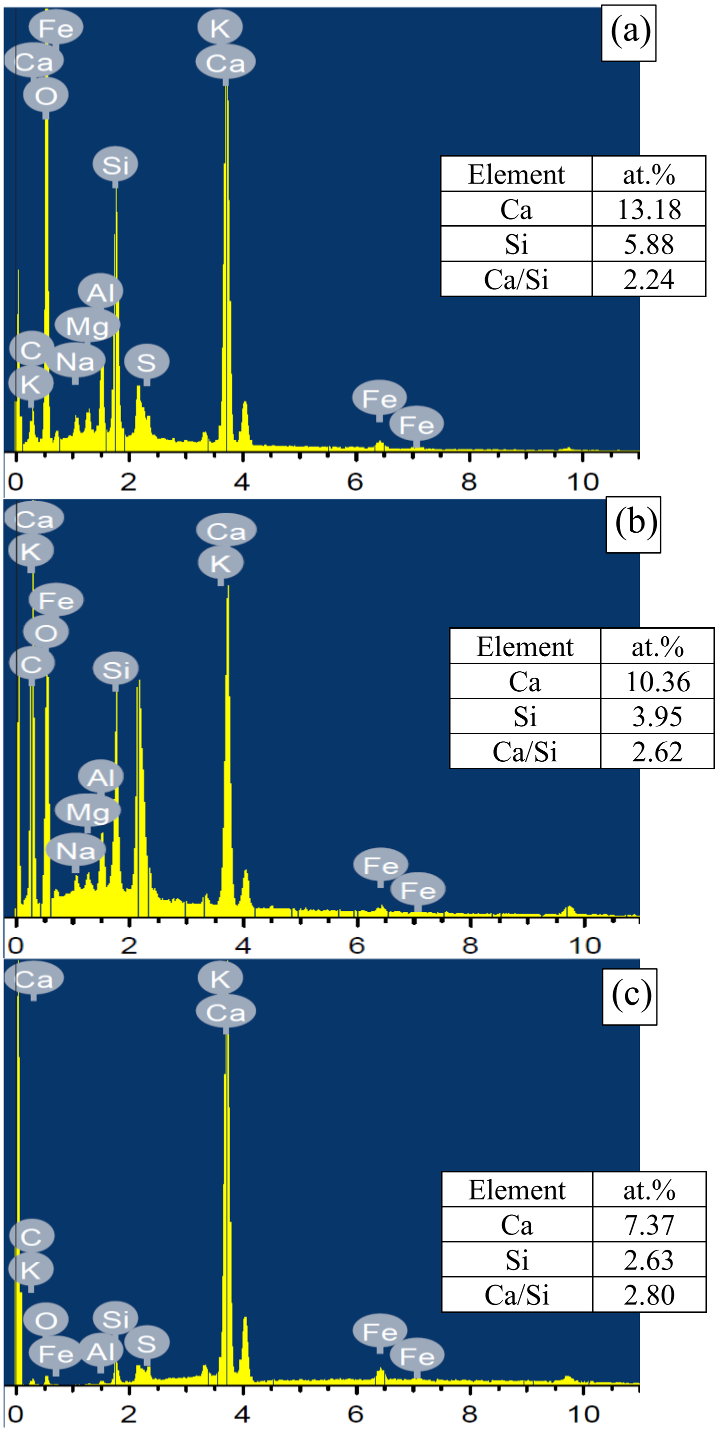

Figure 4.10 EDS images of FA-RCA-NRL concrete at 56 days with 25% fly ash replacement and r/b ratios of (a) 0%, (b) 0.5% (optimal), and (c) 2%

Figure 4.10 presents the EDX spectra of FA-RCA-NRL concretes at 56 days with 25% FA replacement for different r/b ratios. The dominant elements identified across all samples were Ca, Si, and Al, confirming the formation of C-S-H and C-A-S-H phases that govern the strength development of pozzolanic cementitious systems (Tokpatayeva et al. 2022; Wang and Ishida 2019; Wang et al. 2021). In the NRL-free mixture (r/b = 0%), the peaks of Ca, Si, and Al were most prominent, indicating a high degree of cement hydration and active pozzolanic reaction between FA and the liberated calcium hydroxide, which corresponds to the dense microstructure and high compressive strength observed in SEM analysis. As the r/b ratio increased to 0.5% and 2.0%, the relative intensities of Si and Al declined, while the carbon (C) peak-associated with the latex polymer (Rippel et al. 2002) -became increasingly pronounced, reflecting the growing presence of polymer films within the matrix. Quantitative EDX analysis further revealed that the Ca/Si ratio increased from 2.24 in the control mix (r/b = 0%) to 2.62 at r/b = 0.5% and 2.80 at r/b = 2.0%, indicating a progressive shift toward a Ca-rich C-S-H composition and reduced silica incorporation from FA. This trend suggests that higher NRL contents tend to suppress the pozzolanic reaction and the formation of secondary C-S-H, leading to a chemically less refined microstructure. Nevertheless, the r/b = 0.5% mixture, despite its moderately higher Ca/Si ratio, exhibited the greatest compressive, flexural, and fatigue strengths, implying that the physical benefits of latex film formation-such as crack bridging, improved ITZ bonding, and enhanced energy dissipation-can outweigh the less favorable chemical composition at this dosage. Conversely, at r/b = 2.0%, the combination of an excessively high Ca/Si ratio and the porous, polymer-rich morphology observed in SEM images reflects severe hydration inhibition and weakened matrix connectivity, explaining the marked reduction in mechanical and fatigue performance at this dosage.

4.5 CARBON EMISSION AND COST ANALYSES

The life-cycle assessment (LCA) in this study followed a cradle-to-gate system boundary, encompassing raw material extraction, processing, transportation, and concrete production up to the batching stage. The emission factors used for the calculations are summarized in Table 4 and were primarily obtained from published literature sources (McLellan et al., 2011; Ekundayo et al., 2019; Alzard et al., 2020; Usubharatana and Phungrassami, 2018; Kanagaraj et al., 2025). The selected emission values fall within the ranges reported by internationally recognized databases, notably the IPCC (2006) Guidelines (Eggleston et al. 2006; IPCC 2006), thereby confirming their consistency with established life-cycle inventory data for cement, aggregates, and industrial by-products. Consequently, the results represent the embodied carbon of the concrete mixtures, excluding service-life and end-of-life stages. To reflect realistic local production conditions in Thailand, it was assumed that all raw materials were sourced within a 50 km radius of the batching plant and transported by diesel trucks with an average emission factor of 0.10 kg CO_2-e per ton·km. The cost and transport data were based on average 2024 market values in the Nakhon Ratchasima region, including fuel, handling, and delivery. These assumptions ensure that both the emission and cost assessments represent typical regional supply chains under Thai conditions.

Figure 4.11 illustrates the total CO_2-equivalent emissions (kg CO_2-e), material cost (USD/m^3) and fatigue life (cycles at SR = 60%) of seven FA-RCA-NRL concrete mixtures, incorporating FA replacement levels of 0%, 15%, 20%, and 25%, with and without 0.5% NRL. The emissions and material cost were calculated based on the factors for each material, as presented in **Table 4.4**. It should be noted that the comparison in **Figure 4.11** focuses on mixtures with r/b = 0.5%, since this dosage was identified as the optimum latex content. At this level, both f_c and f_f consistently satisfied the minimum requirements for rigid pavement specified by the Department of Highways, Thailand ($f_c \geq 32$ MPa, $f_f \geq 4.2$ MPa), while higher r/b ratios (≥1.0) led to performance reductions below the standard. Therefore, r/b = 0.5% was selected as the representative condition for evaluating the balance among mechanical performance, fatigue resistance, emissions, and material cost.

The results of **Figure 4.11(a)** revealed that cement dominated the carbon footprint, contributing over 98% of total emissions in each mix. The reference mix with FA = 0% (Youromphruk et al. 2025) recorded the highest CO_2 emissions at 402.83 kg CO_2-e. In comparison, as FA content increased 15% to 25%, cement consumption and total CO_2 emissions decreased progressively, with the lowest emission observed in the RCA+25% FA mixture (304.20 kg CO_2-e). The addition of 0.5% NRL marginally increased emissions by about 0.42 kg CO_2-e per mix. For example, RCA+0.5%NRL+15%FA emitted

344.08 kg CO_2-e compared to 343.66 kg CO_2-e for the NRL-free equivalent, and this small increase was consistent across all FA replacement levels. Importantly, if RCA was entirely replaced with natural aggregate (NA) at the same dosage of 1018 kg per cubic meter, the total CO_2 emissions per mix would increase by approximately 35.6 kg CO2-e, highlighting the environmental benefit of using RCA over NA.

Table 4.4 Emission factors (kg CO_2-e/kg) and Material Cost of concrete mix materials

Material	**Emission factor (kg CO_2-e/kg)**	**Material Cost (USD/kg)**
Cement (kg)	0.86 (McLellan et al. 2011)	0.114 (Egemen et al. 2024)
Fly ash (kg)	0.007 (McLellan et al. 2011)	0.0124 (Reiner and Rens 2006)
Sand	0.006 (Ekundayo et al. 2019)	0.0062 (Hamada et al. 2023)
RCA	0.000667 (Alzard et al. 2020)	0.0055 (Prasittisopin et al. 2025)
NRL	0.095 (Usubharatana and Phungrassami 2018)	1.92 (Yaowarat et al. 2021)
NA	0.035 (Kanagaraj et al. 2025)	0.042 (Kanagaraj et al. 2025)

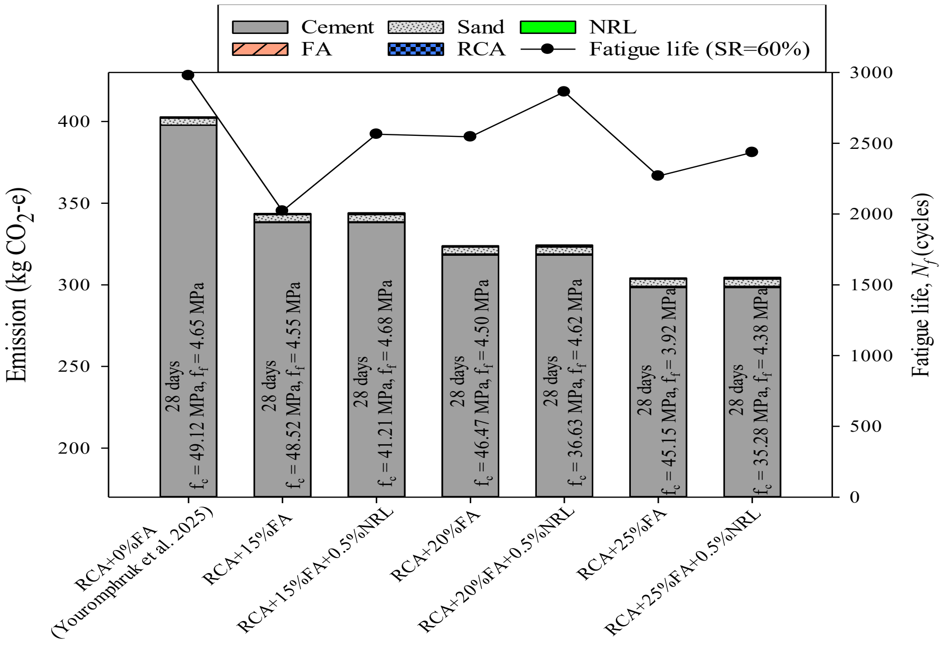

(a)

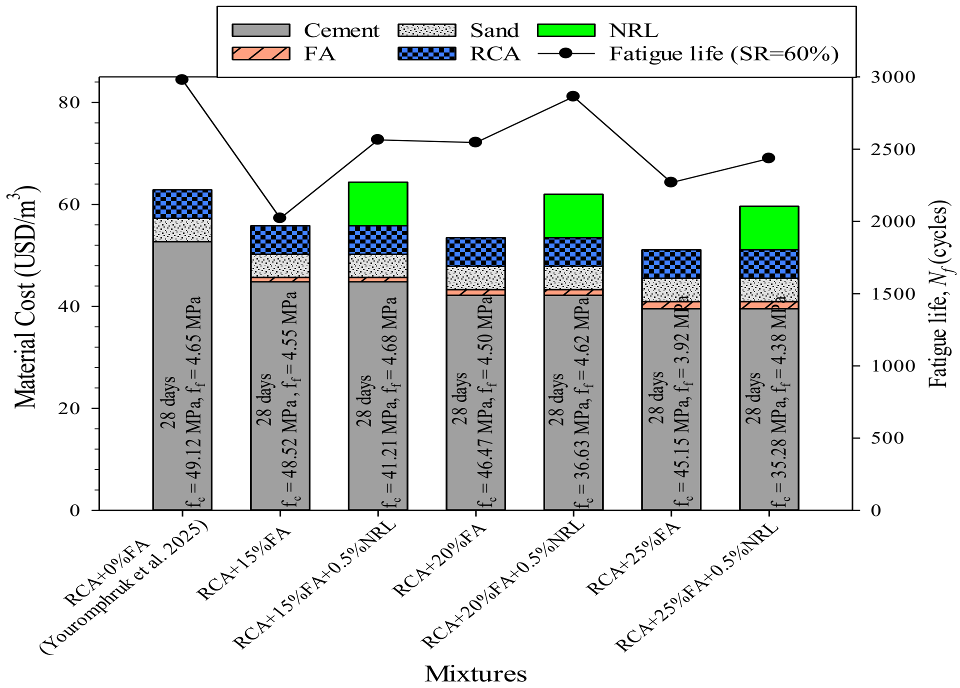

(b)

Figure 4.11 FA–RCA–NRL concrete mixtures and corresponding 28-day compressive strength, flexural strength and fatigue life: (a) CO_2 emissions and (b) material cost.

When engineering performance is considered together with emissions, the results show that flexural strength at 28 days and fatigue life at SR = 60% were broadly comparable among the FA-blended mixtures and the FA = 0% reference. The FA = 0% mix achieved the highest values, with f_f = 4.65 MPa and a fatigue life of 2978 cycles, but at the cost of the largest footprint (402.83 kg CO_2-e). By contrast, FA substitution reduced emissions substantially while maintaining acceptable performance. For example, at 15% FA, the r/b = 0% mix recorded f_f = 4.55 MPa and 2022 cycles, while the addition of 0.5% NRL slightly increased flexural strength (4.68 MPa) and improved fatigue life to 2564 cycles, although emissions rose marginally. At 20% FA, the r/b = 0% mix achieved f_f = 4.50 MPa and 2546 cycles, and with 0.5% NRL, flexural strength remained comparable (4.62 MPa) while fatigue life increased to 2863 cycles, again with only a small emission penalty. At 25% FA, the r/b = 0% concrete recorded lower values (f_f = 3.92 MPa, 2269 cycles), yet the incorporation of 0.5% NRL enhanced both flexural strength (4.38 MPa) and fatigue resistance (2436 cycles), narrowing the gap with the FA = 0% baseline while still achieving the lowest footprint (304.20–304.63 kg CO_2-e).

A similar trend was observed for material cost (**Figure 11(b)**). The FA = 0% reference mix (Youromphruk et al. 2025) recorded the highest cost at 62.87 USD/m³, which can be attributed to its full reliance on cement, the most expensive binder at 0.114 USD/kg. In contrast, partial replacement of cement with FA (unit cost = 0.0124 USD/kg) reduced the overall cost substantially, down to 51.13 USD/m³ for the RCA+25%FA mix. This highlights the strong economic benefit of FA substitution, since FA costs less than one-ninth of cement per kilogram. The addition of NRL, which has the highest unit cost among the considered materials (1.92 USD/kg), increased the total cost of mixtures by about 8–9 USD/m³. For instance, RCA+0.5%NRL+25%FA costs 59.67 USD/m³ compared with 51.13 USD/m³ for RCA+25%FA. This trend was consistent across all FA replacement levels.

In terms of engineering performance, the FA = 0% mixture achieved the highest f_c (49.12 MPa), f_f (4.65 MPa), and N_f (2978 cycles) at 28 days (Youromphruk et al., 2025), outperforming FA-blended concretes. Nevertheless, FA-based mixtures demonstrated only slightly lower strengths (e.g., 48.52 MPa, 4.55 MPa, and 2022 cycles for RCA+15%FA), while offering significant environmental and cost benefits. The addition of NRL improved f_f and N_f at moderate levels (e.g., 4.68 MPa and 2564 cycles for RCA+0.5%NRL+15%FA). However, these benefits came at the expense of higher material cost and a moderate reduction in compressive strength.

These findings emphasize that partial replacement of cement with FA not only reduces the environmental impact but also lowers material cost. For example, CO_2 emissions decreased from 402.83 kg CO_2-e and a cost of 62.87 USD/m^3 in the FA = 0% reference mix to as low as 304.20 kg CO_2-e and 51.13 USD/m^3 in the RCA+25%FA mixture. Although the compressive and flexural strengths of FA-blended concretes (e.g., 45.15 MPa and 3.92 MPa at 28 days for RCA+25%FA) were slightly lower than the FA = 0% baseline (49.12 MPa and 4.65 MPa), the trade-off is offset by substantial sustainability and economic gains. The incorporation of a low dosage of NRL further enhanced flexural strength (e.g., 4.68 MPa for RCA+0.5%NRL+15%FA) but increased costs (to 64.36 USD/m^3) and reduced compressive strength (41.21 MPa). Overall, the compressive and flexural strength values annotated on each bar confirm that FA substitution strikes a favorable balance between lower CO_2 emissions, reduced cost, and adequate mechanical performance, while NRL addition offers flexural benefits at the expense of higher cost and moderate compressive strength loss.

When considering sustainability and economics under the Thai pavement criteria ($f_c \geq 32$ MPa, $f_f \geq 4.2$ MPa), two mixes stand out as optimal choices. For minimizing emissions, the RCA+0.5%NRL+25%FA mix achieved the lowest CO_2 footprint while still meeting the requirements, recording 304.63 kg CO_2-e/m^3, with f_c = 35.28 MPa, f_f = 4.38 MPa, and a cost of 59.67 USD/m^3. In contrast, for minimizing cost, the RCA+20%FA mix offered the most economical option at 53.48 USD/m^3, while also maintaining acceptable environmental and mechanical performance (323.93 kg CO_2-e/m^3, f_c = 46.47 MPa, f_f = 4.50 MPa). These results highlight that RCA+0.5%NRL+25%FA is the most sustainable mix in terms of emissions, whereas RCA+20%FA provides the best balance for cost efficiency.

4.6 CONCLUSION

This study highlights the synergistic effects of fly ash (FA) and natural rubber latex (NRL) on the mechanical, microstructural, and durability performance of RCA-based pavement concrete. Moderate NRL dosages (r/b = 0.5-1.0%) combined with higher FA contents (20-25%) improved flexural strength and fatigue resistance, attributed to thin latex films that bridged microvoids and strengthened the interfacial transition zone. In contrast, excessive NRL (r/b ≥ 1.5%) inhibited hydration, producing a porous, Ca-rich matrix with reduced Si and Al contents as shown by SEM-EDX. The optimum mix (r/b = 0.5%, FA=25%) achieved the best balance of strength, ductility, and fatigue performance for pavement applications.

From a sustainability perspective, cement was the primary source of CO_2 emissions, but this impact was substantially reduced through FA substitution. Increasing FA content progressively lowered both emissions and cost, with RCA+25%FA achieving the lowest cost (51.13 USD/m^3). and the lowest footprint among FA-only mixes. The inclusion of NRL slightly increased emissions (~0.42 kg/m^3) and raised costs by about 8–9 USD/m^3 due to its higher unit price (1.92 USD/kg), as seen in RCA+0.5%NRL+25%FA (59.67 USD/m^3). When considering sustainability and economics under the Thai pavement criteria (f_c ≥ 32 MPa, f_f ≥ 4.2 MPa), two mixes were identified as optimal. The RCA+0.5%NRL+25%FA mix provided the lowest CO_2 footprint (304.63 kg CO_2-e/m^3), with adequate strength (f_c = 35.28 MPa, f_f = 4.38 MPa), and a cost of 59.67 USD/m^3. While the RCA + 20% FA mix offered the most economical solution (53.48 USD/m^3) with balanced environmental and mechanical performance (323.93 kg CO_2-e/m^3, f_c = 46.47 MPa, f_f = 4.50 MPa). Overall, the former is recommended for maximum sustainability, whereas the latter provides the best cost–performance balance for pavement concrete applications. It should be noted that the CO_2 emission and cost analyses are based on local Thai production and transport conditions, and the quantitative results may vary under different regional supply chains or energy systems. Nevertheless, the comparative trends and identified optimal mix proportions remain valid for sustainable pavement concrete design.

4.7 REFERENCES

Accornero, F., Rubino, A., Marano, G.C., Carpinteri, A. (2024). Smart construction of fibre-reinforced concrete structures: size-scale effects on minimum reinforcement and plastic rotation capacity. *Smart Construction and*

Sustainable Cities, 2, 12(2024). Doi: https://doi.org/10.1007/s44268-024-00034-6.

Alzard, M., El-Hassan, H., and El Maaddawy, T. "Development of a life cycle inventory dataset for recycled concrete aggregates in the city of Abu Dhabi." *Proc., International Conference on Civil, Structural and Transportation Engineering*, Avestia Publishing, 227-228.

Arulrajah, A., Disfani, M. M., Haghighi, H., Mohammadinia, A., and Horpibulsuk, S. (2015). "Modulus of rupture evaluation of cement stabilized recycled glass/recycled concrete aggregate blends." *Construction and Building Materials*, 84, 146-155.

Arulrajah, A., Kua, T.-A., Suksiripattanapong, C., and Horpibulsuk, S. (2019). "Stiffness and strength properties of spent coffee grounds-recycled glass geopolymers." *Road Materials and Pavement Design*, 20(3), 623-638.

Awoyera, P. O., Oluyemi, F., Bheel, N., Aluko, O., de Azevedo, A. R., and Olalusi, O. B. (2024). "Morphology and strength of concrete incorporating natural rubber latex and plastic fibers." *Green materials in civil engineering*, Elsevier, 201-217.

Behera, M., Bhattacharyya, S., Minocha, A., Deoliya, R., and Maiti, S. (2014). "Recycled aggregate from C&D waste & its use in concrete–A breakthrough towards sustainability in construction sector: A review." *Construction and building materials*, 68, 501-516.

BSI (1983). "BS 1881-108. Testing Concrete. Method for Making Test Cubes from Fresh Concrete." British Standards Institution London.

Buritatum, A., Horpibulsuk, S., Udomchai, A., Suddeepong, A., Takaikaew, T., Vichitcholchai, N., Horpibulsuk, J., and Arulrajah, A. (2021). "Durability improvement of cement stabilized pavement base using natural rubber latex." *Transportation Geotechnics*, 28, 100518.

Buritatun, A., Takaikaew, T., Horpibulsuk, S., Udomchai, A., Hoy, M., Vichitcholchai, N., and Arulrajah, A. (2020). "Mechanical strength improvement of cement-stabilized soil using natural rubber latex for pavement base applications." *Journal of Materials in Civil Engineering*, 32(12), 04020372.

C39, A. (2021). "Standard test method for compressive strength of cylindrical concrete specimens." *ASTM international West Conshohocken, PA, USA*.

C78, A. "Standard Test Method for Flexural Strength of Concrete (Using Simple Beam with Third-Points Loading." *Proc., ASTM international West Conshohocken, PA, USA*.

C143, A. (2015). "Standard test method for slump of hydraulic-cement concrete." ASTM international West Conshohocken, PA, USA.

C192, A. (2019). "standard practice for making and curing concrete test specimens in the laboratory." *ASTM international West Conshohocken, PA, USA*, 4-9.

C618, A. (2019). "Standard Specification for Coal Fly Ash and Raw or Calcined Natural Pozzolan for Use in Concrete." *ASTM international West Conshohocken, PA, USA*.

Dilbas, H., Şimşek, M., and Çakır, Ö. (2014). "An investigation on mechanical and physical properties of recycled aggregate concrete (RAC) with and without silica fume." *Construction and Building materials*, 61, 50-59.

Egemen, M., Ali, F., and Aydin, E. (2024). "An approach to mixture design and cost analysis for cement pastes composed of class C fly ashes for better sustainable construction." *Buildings*, 14(2), 373.

Eggleston, H., Buendia, L., Miwa, K., Ngara, T., and Tanabe, K. (2006). "2006 IPCC guidelines for national greenhouse gas inventories."

Ekundayo, D., Babatunde, S. O., Ekundayo, A., Perera, S., and Udeaja, C. (2019). "Life cycle carbon emissions and comparative evaluation of selected open source UK embodied carbon counting tools." *Construction economics and building*, 19(2), 220-242.

Elyasigorji, F., Farajiani, F., Hajipour Manjili, M., Lin, Q., Elyasigorji, S., Farhangi, V., and Tabatabai, H. (2023). "Comprehensive review of direct and indirect pozzolanic reactivity testing methods." *Buildings*, 13(11), 2789.

Etxeberria, M., Vázquez, E., Marí, A., and Barra, M. (2007). "Influence of amount of recycled coarse aggregates and production process on properties of recycled aggregate concrete." *Cement and concrete research*, 37(5), 735-742.

Golewski, G. L. (2022). "The role of pozzolanic activity of siliceous fly ash in the formation of the structure of sustainable cementitious composites." *Sustainable Chemistry*, 3(4), 520-534.

Hamada, H. M., Abed, F., Al-Sadoon, Z. A., Elnassar, Z., and Hassan, A. (2023). "The use of treated desert sand in sustainable concrete: A mechanical and microstructure study." *Journal of Building Engineering*, 79, 107843.

Han, S., Wang, Y., Wang, Q., Han, L., and Han, G. (2024). "Film-formation processes of polymer emulsions in polymer-cement waterproof coatings and their effect on coatings' macroscopic properties." *Construction and Building Materials*, 438, 137137.

Hertwich, E. G., and Peters, G. P. (2009). "Carbon footprint of nations: a global, trade-linked analysis." *Environmental science & technology*, 43(16), 6414-6420.

Hoy, M., Tran, N. Q., Suddeepong, A., Horpibulsuk, S., Buritatum, A., Yaowarat, T., and Arulrajah, A. (2023). "Wetting-drying durability performance of cement-stabilized recycled materials and lateritic soil using natural rubber latex." *Construction and Building Materials*, 403, 133108.

Hoy, M., Tran, N. Q., Suddeepong, A., Horpibulsuk, S., Mobkrathok, M., Chinkulkijniwat, A., and Arulrajah, A. (2023). "Improved fatigue properties of cement-stabilized recycled materials–Lateritic soil using natural rubber latex for sustainable pavement applications." *Transportation Geotechnics*, 40, 100959.

IPCC, I. P. O. C. C. (2006). "THE IPCC." IGES Japan.

Jansen, D., Neubauer, J., Goetz-Neunhoeffer, F., Haerzschel, R., and Hergeth, W.-D. (2012). "Change in reaction kinetics of a Portland cement caused by a superplasticizer—Calculation of heat flow curves from XRD data." *Cement and Concrete Research*, 42(2), 327-332.

Kanagaraj, B., Anand, N., Alengaram, U. J., Raj, R. S., and Lubloy, E. (2025). "A Comprehensive Review on Life-cycle assessment of concrete using industrial by-products." *Case Studies in Chemical and Environmental Engineering*, 101260.

Kang, S.-H., Kang, H., Lee, N., Kwon, Y.-H., and Moon, J. (2022). "Development of cementless ultra-high performance fly ash composite (UHPFC) using nucleated pozzolanic reaction of low Ca fly ash." *Cement and Concrete Composites*, 132, 104650.

Kang, S., Kim, J., Moon, C., and Song, M. (2015). "Early hydration-retarding mechanism of polymer-modified cement." *Materials Research Innovations*, 19(sup8), S8-22-S28-26.

Knapen, E., and Van Gemert, D. (2015). "Polymer film formation in cement mortars modified with water-soluble polymers." *Cement and Concrete Composites*, 58, 23-28.

Lazarevic, D., and Martin, M. (2016). "Life cycle assessments, carbon footprints and carbon visions: Analysing environmental systems analyses of transportation biofuels in Sweden." *Journal of cleaner production*, 137, 249-257.

Li, G., Morlor, C. S., Leung, C., and Wang, H. (2021). "Mechanical properties and fractal analysis of cement mortar incorporating styrene-butadiene rubber latex and carboxylated MWCNTs." *Construction and Building Materials*, 309, 125175.

McLellan, B. C., Williams, R. P., Lay, J., Van Riessen, A., and Corder, G. D. (2011). "Costs and carbon emissions for geopolymer pastes in comparison to ordinary portland cement." *Journal of cleaner production*, 19(9-10), 1080-1090.

Naseem, Z., Shamsaei, E., Sagoe-Crentsil, K., and Duan, W. (2023). "Microstructural and polymer film interaction mechanisms: Insights of GO-reinforced polymer-modified cement composites." *Journal of Building Engineering*, 80, 107962.

Nhieu, D. V., Hoy, M., Horpibulsuk, S., Karntatam, K., Arulrajah, A., and Horpibulsuk, J. (2023). "Cement–natural rubber latex stabilised recycled concrete aggregate as a pavement base material." *Road Materials and Pavement Design*, 24(6), 1636-1650.

Omary, S., Ghorbel, E., and Wardeh, G. (2016). "Relationships between recycled concrete aggregates characteristics and recycled aggregates concretes properties." *Construction and Building Materials*, 108, 163-174.

Park, S.-M., Jang, J.-G., Chae, S.-A., and Lee, H.-K. (2016). "An NMR spectroscopic investigation of aluminosilicate gel in alkali-activated fly ash in a CO2-rich environment." *Materials*, 9(5), 308.

Plank, J., Sakai, E., Miao, C., Yu, C., and Hong, J. (2015). "Chemical admixtures— Chemistry, applications and their impact on concrete microstructure and durability." *Cement and concrete research*, 78, 81-99.

Prasittisopin, L., Tuvayanond, W., Kang, T. H.-K., and Kaewunruen, S. (2025). "Concrete mix design of recycled concrete aggregate (rca): analysis of review papers, characteristics, research trends, and underexplored topics." *Resources*, 14(2), 21.

Reijnders, L. (2012). "Life cycle assessment of greenhouse gas emissions." *Handbook of climate change mitigation*, Springer, 13-41.

Reiner, M., and Rens, K. (2006). "High-volume fly ash concrete: analysis and application." *Practice periodical on structural design and construction*, 11(1), 58-64.

Rippel, M. M., Paula Leite, C. A., and Galembeck, F. (2002). "Elemental mapping in natural rubber latex films by electron energy loss spectroscopy associated with transmission electron microscopy." *Analytical chemistry*, 74(11), 2541-2546.

Silva, R., De Brito, J., and Dhir, R. (2014). "Properties and composition of recycled aggregates from construction and demolition waste suitable for concrete production." *Construction and Building Materials*, 65, 201-217.

Smith, K. D., and Roesler, J. R. (2004). "Review of fatigue models for concrete airfield pavement design." *Airfield pavements: Challenges and new technologies*, 231-258.

Stirewalt, T. F.-N. (2021). *Cracking Causes and Resistance in Very Early Strength Latex Modified Concrete Overlays with and Without Nonmetallic Fibers*, North Carolina State University.

Sukmak, G., Sukmak, P., Horpibulsuk, S., Yaowarat, T., Kunchariyakun, K., Patarapaiboolchai, O., and Arulrajah, A. (2020). "Physical and mechanical properties of natural rubber modified cement paste." *Construction and Building Materials*, 244, 118319.

Tokpatayeva, R., Castillo, A., Yoon, J., Kaladharan, G., Jafari, K., Arachchige, R. M., Rajabipour, F., Peethamparan, S., and Olek, J. (2022). "Comparative study of the reactivity and performance of different nontraditional and natural pozzolans in cementitious system." *Advances in Civil Engineering Materials*, 11(2), 670-693.

Tran, N. Q., Hoy, M., Suddeepong, A., Horpibulsuk, S., Kantathum, K., and Arulrajah, A. (2022). "Improved mechanical and microstructure of cement-stabilized lateritic soil using recycled materials replacement and natural rubber latex for pavement applications." *Construction and Building Materials*, 347, 128547.

Usubharatana, P., and Phungrassami, H. (2018). "Carbon footprints of rubber products supply chains (fresh latex to rubber glove)." *Applied Ecology & Environmental Research*, 16(2).

Wang, Q., Wang, Y., Han, S., Han, L., and Han, G. (2023). "Hydration behaviour of cement in polymer cement waterproof coating and its effect on the macroscopic performance." *Construction and Building Materials*, 408, 133825.

Wang, T., and Ishida, T. (2019). "Multiphase pozzolanic reaction model of low-calcium fly ash in cement systems." *Cement and Concrete Research*, 122, 274-287.

Wang, T., Ishida, T., Gu, R., and Luan, Y. (2021). "Experimental investigation of pozzolanic reaction and curing temperature-dependence of low-calcium fly ash in cement system and Ca-Si-Al element distribution of fly ash-blended cement paste." *Construction and Building Materials*, 267, 121012.

Werkmeister, S., Dawson, A., and Wellner, F. (2004). "Pavement design model for unbound granular materials." *Journal of Transportation Engineering*, 130(5), 665-674.

Yaowarat, T., Horpibulsuk, S., Arulrajah, A., Mirzababaei, M., and A Rashid, A. S. (2018). "Compressive and flexural strength of polyvinyl alcohol–modified pavement concrete using recycled concrete aggregates." *Journal of Materials in Civil Engineering*, 30(4), 04018046.

Yaowarat, T., Horpibulsuk, S., Arulrajah, A., Mohammadinia, A., and Chinkulkijniwat, A. (2019). "Recycled concrete aggregate modified with polyvinyl alcohol and fly ash for concrete pavement applications." *Journal of Materials in Civil Engineering*, 31(7), 04019103.

Yaowarat, T., Suddeepong, A., Hoy, M., Horpibulsuk, S., Takaikaew, T., Vichitcholchai, N., Arulrajah, A., and Chinkulkijniwat, A. (2021). "Improvement of flexural strength of concrete pavements using natural rubber latex." *Construction and Building Materials*, 282, 122704.

Ye, P., Chen, Z., and Su, W. (2022). "Mechanical properties of fully recycled coarse aggregate concrete with polypropylene fiber." *Case Studies in Construction Materials*, 17, e01352.

Youromphruk, C., Yaowarat, T., Horpibulsuk, S., Buritatum, A., Suddeepong, A. P., Veena; , Hoy, M., and Arulrajah, A. (2025). "Enhancing the Flexural strength of concrete pavements with recycled aggregate using natural rubber latex additive." *Journal of Materials in Civil Engineering*, Accepted February 21, 2025.